Iraqi National Journal of Earth Science

www.earth.mosuljournals.com

Implications for Geochemistry of the Egyptian Clay Deposits and their Suitability for the Vitrified Clay Pipes Industry

Hatem M. El-Desoky[1], Ahmed Wahid[2], Osama R. El-Shahat [3]

[1,3] *Department of Geology, Faculty of Science, Al-Azhar University, Egypt.*

[2]*Quality Control Manager, Sweillem Vitrified Clay Pipes Company*

Article information

Received: 28- Aug -2022

Accepted: 27- Nov -2022

Available online: 31-Dec-2022

Keywords:
Clays
shales
geochemical
weathering effect
firing
vitrified clay pipes

Correspondence:
Name: Ahmed Wahid
awahid_84@sweillem.net

ABSTRACT

Combined geology, mineralogy, and geochemical data of some Egyptian clay minerals have been proved to be a powerful tool in evaluating these clay deposits for the vitrified clay pipes industry. Representative samples underwent mineralogical and geochemical analysis involving major and trace element analyses. A geochemical study of the clay deposits from different formations in Egypt is carried out to determine the environmental deposition, provenance, chemical index of alteration, and paleo-oxygenation conditions. Mineralogical studies using X-ray diffraction analysis reveal prominent kaolinite, montmorillonite, and illite peaks; harmful accessory minerals include quartz, hematite, halite, calcite, and dolomite. The total silica content is high in Mendishia, Monkar El-Wahsh, Bahariya, Wadi Natrun, Sebaya, Gabal Hamza, and Qasr El-Sagha clay deposits, while Heiz and Arish clay deposits have lower silica content. The studied clay deposits are characterized by high alumina (11.5% to 18.3%) and silica (45.6% to 60.2%) contents. The CaO and MgO are high in Heiz and Arish clay deposits which implies that carbonates are present. They are characterized by very high Fe_2O_3, Ba, Sr, and Zr as well as low K_2O, Ni, Cu, Zn, Rb, Y, Pb, Ga, and Nb contents. The Heiz and Arish clay deposits characterized by high content of Na_2O. The studied characteristics are relevant for the properties of vitrified clay pipes and that three clay deposits of (Heiz, Gabal Hamza, and Monkar El-Wahsh clay deposits) exhibit the required characteristics.

DOI: 10.33899/earth.2022.135553.1029,

دراسات جيوكيميائية وتطبيقية على رواسب الطين المصرية ومدى ملاءمتها لصناعة الأنابيب الفخارية المزججة

حاتم محمد عبدو الدسوقي [1]، أحمد وحيد [2]، أسامة رمزي الشحات [3]

[1، 3] قسم علوم الأرض، كلية العلوم، جامعة الأزهر، مصر

[2] مدير مراقبة الجودة ، شركة سويلم للأنابيب الفخارية

معلومات الارشفة

تاريخ الاستلام: 28-أغسطس-2022

تاريخ القبول: 27-نوفمبر-2022

تاريخ النشر الالكتروني: 31-ديسمبر-2022

الكلمات المفتاحية:

خامات الطين

جيوكيمياء

تاثير التجوية

مواسير الفخار الحجرى

المعالجة الحرارية

المراسلة:

الاسم: أحمد وحيد

awahid_84@sweillem.net

الملخص

أثبتت البيانات الجيولوجية وعلم المعادن والجيوكيميائية المجمعة لبعض معادن الطين المصرى أنها أداة قوية فى تقييم هذه الرواسب الطينية لصناعة الأنابيب الفخارية المزججة. خضعت العينات التمثيلية لتحليل معدنى وجيوكيميائى تضمن تحليلات رئيسية وتحليلات للعناصر النزرة. تم إجراء دراسة جيوكيميائية لرواسب الطين من التكوينات المختلفة فى مصر لتحديد الترسب البيئى، والأصل، والمؤشر الكيميائى للتغير وظروف الأكسجة القديمة. كشفت الدراسات المعدنية باستخدام تحليل حيود الأشعة السينية عن قمم بارزة من الكاولينيت، والمونتموريلونيت، والقمم المضيئة؛ تشمل المعادن الملحقة الضارة الكوارتز والهيماتيت والهاليت والكالسيت والدولوميت. المحتوى الكلى للسيليكا مرتفع فى منديشية ومنكار الوحش والبحرية ووادى النطرون وسيباية وجبل حمزة وقصر الصاغة بينما تحتوى رواسب طينية هيز والعريش على نسبة أقل من السيليكا. تميزت الرواسب الطينية المدروسة بمحتويات عالية من الألومينا (11.5٪ إلى 18.3٪) والسيليكا (45.6٪ إلى 60.2٪). يحتوى كل من CaO و MgO على نسبة عالية من رواسب طين Heiz و Arish مما يدل على وجود الكربونات. تتميز بمحتويات عالية جدًا من Fe_2O_3 و Ba و Sr و Zr ومنخفضة فى محتويات K_2O و Ni و Cu و Zn و Rb و Y و Pb و Ga و Nb. يتم عرضها من خلال ارتفاع Na_2O فى رواسب طينية Heiz و Arish. تم إجراء العديد من المحاولات فى هذا المجال مثل الانكماش وامتصاص الماء والكثافة الظاهرية ومعامل النشوة والمسامية الظاهرة والمقاومة الكيميائية فى هذا المجال لدراسة تأثيرها على خصائص الأنابيب الفخارية المزججة.

DOI: 10.33899/earth.2022.135553.1029,

Introduction

Shale represents the most abundant type of sediment in the sedimentary basins worldwide (Pettijohn, 1975) and is considered to represent average crustal provenance composition much better than any other detrital sedimentary rocks (McCulloch and Wasserburg, 1978). The present investigation focuses on the mineralogical, geochemical, and technological characteristics of some Egyptian clay deposits to establish its suitability for the vitrified clay pipes industry (Fig.1).

Egyptian clay deposits are distributed in West Central Sinai in the Carboniferous sediments (Abu Natash, Nukhl, and Budra regions). They are confined to the Nubia Formation in the regions of Aswan, Wadi Araba (Abu Darag), and West Central Sinai (Moussaba Salama, Dehisa, Farsh El-Gozlan). In the Nile Valley between Idfu and Qena, montmorillonite - beidellite clays are encountered in the Dakhla Formation of the Upper Cretaceous age. In the Miocene and Middle and Upper Eocene sediments, clays are also

found. The Recent alluvial loams and silty clays of the Nile flood plain are also among the clay deposits in Egypt.

Prospecting for clay deposits is carried out in the following regions (Fig.2):

i- The Nile Valley (in the area of Aswan and to the south of Cairo)

ii- South of Suez

iii- West Central Sinai

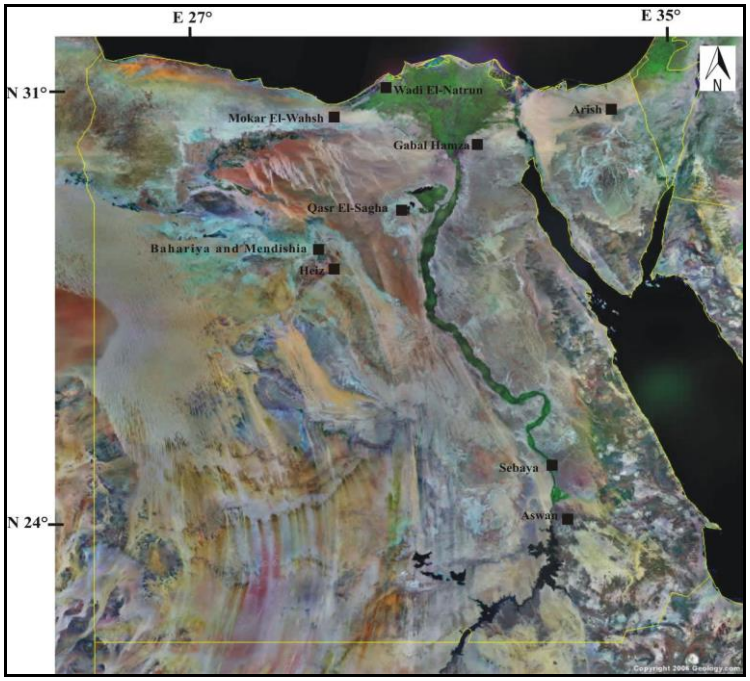

Fig.1. Landsat location map of the studied shale-bearing clay deposits in Egypt.

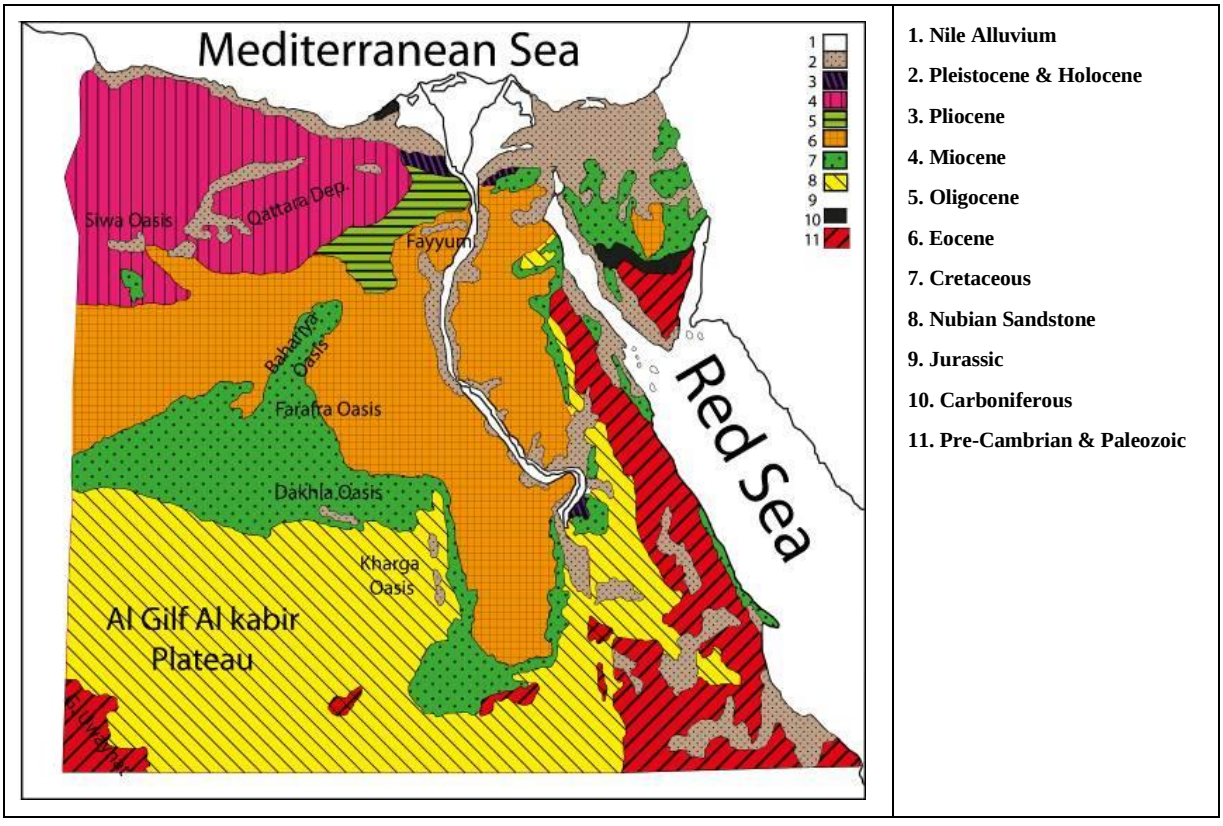

Fig.2. The geological Formations of Egypt (modified after Abu Al-Izz, 1971).

Other locations of shale-bearing clay deposits were mainly investigated by the Salzgitter Company and the following paragraphs are based on the report submitted by this company.

Moussaba Salama clay deposits are located 14 km northeast of the village of Abu Zenima on the left side of Wadi Tayiba. They represent a separate tectonic block of the Nubia Formation at the base of the exposed clays.

Abu Natash clay deposits are located 23 km southeast of Abu Zenima port on the left slope of Wadi Abu Natash. The deposits are confined to the upper succession of the Carboniferous sandy sediments containing basalt sheets and is intensively complicated by tectonic dislocations. Three clay beds varying in thickness up to 1.5-2 m are distinguished in this deposit. The upper two beds are formed of greyish-white slightly ferruginous kaolin. They are suitable for the ceramic industry. From the chemical point of view, they can be used for the production of alumina, but their limited reserves stand against their utilization in this industry.

Wadi Kenaiya clays are similar to those of Abu Natash deposits.

Up to three beds of silty kaolin clays may be distinguished among the sandy sediments of the Upper Carboniferous in the localities of Tayiba, Khaboba, and Wadi Sidra. The main bed is 10-12 m thick. Its upper four meters are formed of silty clays of grey and dark grey color. In its lower part, it is represented by dark grey to black laminated clays. These clays can be used for the production of crude ceramics, except those of Tayiba which can be also utilized for the production of refractories.

The mineralogical analysis of clay deposits relevant to clay pipes industry should be mainly kaolinite and illite, other clay minerals as montmorillonite shouldn't exceed 20 percent of the total clay minerals. The oxides related to the carbonate material (CaO and MgO) shouldn't exceed 10 %. The physical properties after thermal treatment also should have definite values according to manufacturing limits or international standard.

Geology of the studied clay deposits

Heiz clay deposits

Heiz Formation laying on top of the Bahariya Formation in the scraps of the Oasis and some of the isolated hills in the northern part of the depression is composed of a succession of clastics with carbonate interbeds and a dolostone bed at the top, and dolomitic sandstone at the base named the Heiz Formation. The maximum exposed thickness of the Heiz Formation is 30 m. The contacts with both the underlying Bahariya and the overlying Hefhuf Formation are marked by angular unconformities.

The lithofacies and fossil content common in the Heiz Formation indicate shallow marine conditions of deposition with a good supply of clastics from nearby landmasses. Both the Bahariya and the Heiz formations are close to the history of the Cenomanian in the area of the Bahariya – Farafra Facies. This history seems to extend beyond the outcropping sediments since Said (1962) added 725 m clastics in the subsurface to the already exposed 170 m, thus a total thickness of 895 m is estimated for the Bahariya Formation and the interested bed has no overburden.

El-Sebaya clay deposits

Dakhla Formation represents the topmost Cretaceous unit within the Nubia – Abu Ballas Facies. Only the lower part of the formation belongs to the Cretaceous (Maastrichtian), and its upper part is of the Early Paleocene age. The Dakhla covers a part of the plain west of the Nile and a part of Sin El-Kaddab scrap, it extends from Gabal Garra in the north passing by Kurkur Oasis, Gabal Kalabsha, Dungul Oasis and follows the many indications and bends in this scrap (Issawi, 1969). From Kharga it makes the scraps at Abu Tartur and further west at Dakhla Oasis.

The Cretaceous part of the Dakhla Formation is mostly shale with mudstone bands at its lower part in the east and sandstone beds in Darb El-Arabian. In all its southern outcrops, the Dakhla Formation unconformably overlies the Quseir Clastics Member. Only at Beris – Kharga Oasis, the Duwi Formation begins to appear in the section between the two units. At Darb El-Arabian, very thin lenses of phosphate carrying the same Duwi Formation fossils were recorded by Issawi (1971) and Issawi and Fahmy (1975), between the Nubia and Dakhla Formations. In the south of the Darb El Arabian, the Dakhla Formation is replaced by the Shab Clastic Member.

The thickness of the Cretaceous Dakhla Formation is 70 to 120 m in the east to less than 40m at many places in Darb El-Arabian.

The lithology and fossils content of the Dakhla Formation point to the deep marine environment in the east towards the Nile, away from the neritic zone and probably along the fringe of the bathyal zone. The presence of mudstone and sandstone beds points to shallow neritic to littoral environments. The reefal limestone near the top of the formation indicates shallower conditions initiating simply the unconformity at the top of the Maastrichtian section.

In general, the western sections in these facies are shallower with many conglomeratic bands and sandstone beds. East of the Nile, the Dakhla Formation is missing or its place is taken by sandstones on top of the Nubia Formation, the identification of one unit from the other is rather difficult and the interested bed has no overburden.

Bahariya and Mendishia clay deposits

Bahariya Formation covers the floor of the Bahariya Oasis as well as part of the cliffs surrounding the depression. It also builds most of the isolated hills in the central and southern parts of the depression. The thickness of the Bahariya Formation varies from a few meters at the western scrap to 170 m at Gabal El-Dist. The base is not exposed whereas a limestone bed of the Heiz Formation covers its top.

Lithologically, the formation consists of friable, false-bedded variegated sands and sandstones with hard dark brown ferruginous bands. Some of the sandstones are micaceous and gypseous. Stromer (1914) noticed in the Bahariya beds a mixture of marine and land fossils and the interested bed has no overburden.

Qasr El-Sagha clay deposits

Qasr El-Sagha Formation is strikingly developed in the north of Fayoum, where it forms a bold escarpment of great length, consisting of an alternating series of very fossiliferous clays and limestones with sands and sandstones in the upper beds, of a total thickness of 175 m (Beadnell, 1905). The Qasr El-Sagha Formation is distinguished from the conformably underlying Birket Qurun Formation???? by its greater properties of sandstone, sandy mudstone, and carbonaceous shale. From the overlying Gabal Qatrani Formation, the Qasr El-Sagha Formation differs in the absence of variegated beds and gravels and its greater proportion of limestone and shale.

The Qasr El-Sagha Formation is present beneath some of the extensive series separating the Fayoum and the Bahariya depressions and is exposed in the upper part of the eastern escarpment of the later depression and the interested bed has no overburden.

Wadi Natrun clay deposits

Wadi Natrun Formation includes the marine carbonate-shale sequence of the Middle Jurassic age. The carbonates of the section are mostly dolomitic and are more frequent in the upper part of the section. The formation rests unconformably over the basement or the Paleozoic or conformably over the Bahrein Formation.

The Wadi Natrun Formation is always overlain by the Khatatba Formation. The age of this formation is Middle Jurassic. The Wadi Natrun Formation has a limited distribution and

is known only in the eastern part of the north Western Desert, Wadi Natrun, and surroundings. The Wadi Natrun Formation can be probably equated with the Rajabia Formation in Gabal Magha Facies and the interested bed has no overburden.

Arish clay deposits

Esna Formation is distinguished by a section of marl and green shale, enclosing carbonate intercalations, exposed along the scraps in north Kharga and Farafra and the El-Kharafish plateau. It lies between the two carbonate units, the Tarawan Formation at the base and the Thebes Group at the top.

In Kharga, it decreases in thickness from north to south, from a maximum of 160 m to the east of Umm El-Ghanayim to 45 m to the east of Gaga. South of Gaga, it merges into the Garra Formation, whereas its upper part passes into the shale part at the base of the Dungul Formation.

In the Abu Tartur-El-Kharafish plateau areas, the Esna Formation shows the same lithology and lateral changes as the Garra Formation and the interested bed has no overburden.

Gabal Hamza clay deposits (Cairo-Ismailia Road)

Gabal Hamza- Gabal Um Qamar area lies north of the Cairo-Ismailia Desert Road, about 32 km from Cairo. The oldest rocks exposed in the area are of Oligocene age, represented by gravels, sand, and sandstone with scattered silicified wood fragments and small outcrops of weathered basalt sheets. The Oligocene is overlain unconformably by lower Miocene sediments composed of sand and sandstone interbedded by claystone beds, with lateral changes into carbonate facies in the direction of Um Qamar, north of Gabal Hamza. The lower Miocene sediments are unconformably overlain by middle Miocene deposits composed of sandy limestone and dolostone interbedded with some clay. Both the lower and middle Miocene sediments have been considered marine facies deposited in a shallow sub-littoral to the reefal environment (Abdel Wahab and El-Belassy, 1987). Unconformable deposits of upper Miocene age overlying the middle Miocene beds are composed mainly of gravels and sand and are considered non-marine facies. The smectitic clays sampled in the present work came from the lower Miocene and the interested bed has no overburden.

Monkar El-Wahsh clay deposits

The Daba'a Formation is of uniform thickness in the northwestern desert. It is made up of light grey to greenish grey shales with thin beds of limestone. The formation rests on the Apollonia Formation with a minor disconformity and is conformably overlain by the lower Miocene sediments. The environment of deposition was an inner shelf to the littoral, which became estuarine towards the top in many areas. Toward the south, the Daba'a Formation grades laterally into the well-known littoral to deltaic deposition of the Gabal Qatrani Formation (Hantar, 1990). The maximum thickness recorded, however, in the north Western Desert boreholes is 828 m, but over the rest of the area, the thickness ranges from 200 to 400 m. the lower 33 m of the Daba'a Formation in its type section are of late Eocene age, while the upper 209 m belong to the Oligocene and the interested bed has no overburden.

Aswan clay deposits

Rocks of the Aswan region belong to the Nubia Formation. Issawi (1969), Wycisk (1987), and Hendriks et al. (1987) indicated that the Aswan area consists of a thick sedimentary section of Nubian Sandstone Formation of Upper Cretaceous age that overlies the Precambrian basement rocks. This section consists of ferruginous sandstone, sandstone, and clays. Clays are present as beds and lenses of widely varying dimensions within the sandstone beds and the interested bed has an overburden from 3 to 6 meters of red sandstone.

Experimental tests and methodology Materials and Tests

Raw materials testing

Ten composite clay deposit samples from different localities in Egypt are investigated for their composition and properties.

The mineralogical composition is determined by X-ray diffraction analysis using Philips PW 1140/90 X-ray apparatus Cu-k alpha radiation, nickel filter. Interpretation of the diffraction patterns is based on the presence of diffraction peaks of each crystalline species in the sample. The intensity and sharpness of the peaks are affected by the concentration of the crystalline species, fineness of the crystals, crystal imperfections, and the presence of amorphous materials.

The clay fraction of each argillaceous sample (with particle size less than 2 microns) is separated from the bulk sample for clay-mineral identification by decantation and then mounted on a substrate of glass slides (Bish and Reynolds, 1989; Hughes *et al*., 1994) to obtain three patterns. The clay fraction should be analyzed in:

1. Air dried condition (untreated oriented specimen, no treatment was carried out).
2. Heated condition (the oriented specimen is heated to 550° C at a controlled furnace for 2 h).
3. Glycerol-solvated condition (the oriented specimen is exposed to glycerol vapor in a desiccator at 60° C overnight.

Interpretation of the diffraction patterns is based on the presence of diffraction peaks of each crystalline species in the sample. The intensity and sharpness of the peaks are affected by the concentration of the crystalline species, fineness of the crystals, crystal imperfections, and the presence of amorphous materials.

The criteria for identification of the clay and accessory minerals are:

Kaolinite gives strong reflection at angles corresponding to 7.16A° and 3.57A° in the Mg-saturated air-dried samples which remains constant in the other treatments and disappear upon heating at 550°C for four hours. Montmorillonite (Smectite) exhibits a basal reflection (001) at about 14.0-14.5A° for Mg-saturated and air-dried sample which expands to 17.8A° by adding glycol solution and shifts to 10.0A° after K-saturation and heating at 550°C for four hours.

Illite (Hydrous mica) gives diffraction peaks at angles corresponding to 9.96-10.28A° in the Mg-saturated air-dried sample.

Quartz usually gives two fairly strong peaks at angles corresponding to 3.35 and 4.26A°.

The Chemical analysis of composite shale samples are carried out to determine the type and percentage of the major oxides present in the examined samples using X-ray fluorescence (XRF).

Another technique used to identify the clay minerals and to detect the temperature of recrystallization during firing is differential thermal analysis (DTA) using NETZSCH GERATEBAU DILATOMETER 402 EP, GERMANY.

Caliper (vernier) model MITUTOYO DIGITAL CALIPER 0-300 MM, JAPAN, is used to measure the shrinkage of samples after firing and digital balance to weigh the model of the raw material BEL ENGINEERING E- BALANCE 3-DIG-6500G.

The studied shale samples are grinded from bolder size to 8 mm grain size using jaw crusher model RETSCH JAW CRUSHERS BB-200 GERMANY, then using RETSCH-ROTOR BEATER MILLS SR-200, GERMANY to reduce the grain size less than 2 mm.

The plasticity of the shale samples is measured by the Pfefferkorn method, a defined sample with a diameter of 33 mm and an initial height of 40 mm produced either manually or by extrusion is deformed by a free-falling plate with a mass of 1.192 kg.

The apparatus used in the study of the dehydration properties of the investigated shales (TGA) consists of an electric furnace, thermo balance, and automatic recording instrument. Exactly 1 gm of the finely grained sample is weighed to carry out the dehydration process. The rate of heating chosen is 100º C/min and the temperature is raised up to 1000ºC.

Assessment of the material properties after thermal treatment

The samples are fired in a lab kiln (Nanetti – Italy) at a temperature of 1200°C and a soaking time of 2 hours). The texture of the ceramic body fired at 1200°C is shown by Scanning Electron Microscope using SEM Model Quanta 250 FEG (Field Emission Gun) attached with EDX Unit (Energy Dispersive X-ray Analyses), with accelerating voltage 30 kV, 14x magnification up to 1000000, and resolution for Gun.1n. FEI Company, Netherlands.

Physical and mechanical properties of tested samples namely linear shrinkage, porosity, water absorption, bulk density, apparent porosity, modulus of rapture, and chemical resistance are established.

The crystallization of the base vitrified clay pipes is derived from the Egyptian clay deposits. The type and nature of the developed phases and microstructures concerning the parameters of crystallization (temperature and time) of the Egyptian clay deposits are carried out. The effect of heat treatment and the named nucleation catalysts is obvious on thermal expansion or thermal shrinkage of the resultant vitrified clay pipes.

Results

Mineralogy of the studied clay deposits

The X-ray diffraction analysis of the studied clay deposits shows that Heiz clay deposits are composed of kaolinite and quartz (Fig. 3A and B). El-Sebaya clay deposits are composed mainly of kaolinite, montmorillonite, hematite, halite, and quartz (Fig.3C and D). Bahariya clay deposits are composed of kaolinite, halite, and quartz (Fig.3E and F). Mendishia clay deposits are composed of kaolinite, montmorillonite, calcite, dolomite, halite and quartz (Fig.3G and H). Qasr El-Sagha clay deposits are composed of kaolinite, calcite, halite, and quartz (Fig. 4A and B). Wadi Natrun clay deposits are composed of kaolinite, montmorillonite, halite, and quartz (Fig.4C and D). Arish clay deposits are composed of kaolinite, montmorillonite, and quartz (Fig.4E and F). Gabal Hamza clay deposits are composed of kaolinite, illite, and quartz (Fig. 5A and B). Monkar El-Wahsh clay deposits are composed of kaolinite, calcite, dolomite, and quartz (Fig. 5C and D). Aswan clay deposits are composed of kaolinite, montmorillonite, illite, and quartz (Fig. 5E and F).

Geochemistry of Egyptian clay deposits

The ten samples representing the clay deposits are chemically analyzed for their major and trace elements. Geochemical analysis data of the studied clay deposits are given in Tables (1 and 2). Table (1) shows clearly that the total silica content is high in Mendishia, Monkar El-Wahsh, Bahariya, Wadi Natrun, Sebaya, Gabal Hamza, and Qasr El-Sagha clay deposits while Heiz and Arish clay deposits have lower silica content. This is mainly due to the presence of appreciable amounts of free silica in these clay deposits.

The dominantly clay-associated elements, namely combined silica (as silicate), $A1_2O_3$, K_2O, Fe_2O_3, and MgO, are higher in the studied clay deposits.

From the obtained results, the following characteristics of the studied clay deposits can be given:

1) They possess high alumina (11.5% to 18.3%) and silica (45.6% to 60.2%) contents.

2) The CaO and MgO are high in Heiz and Arish clay deposits which implies that carbonates are present.

3) They are characterized by high content of Fe_2O_3, Ba, Sr, and Zr as well as low K_2O, Ni, Cu, Zn, Rb, Y, Pb, Ga, and Nb contents.

4) They are exhibited by high Na_2O in Heiz and Arish clay deposits.

Physical properties

Table 3 shows the values of water absorption of the studied clay samples which indicates that the values range from 0.56% in Heiz sample to 42.9% in Arish sample, the apparent porosity values range from 1.37% in Heiz samples to 36.72% in Arish sample, the bulk density values range from 0.86% in Arish sample to 2.49% in Gabal Hamza sample, the

MOR values range from 4.36 N/mm^2 in Arish sample to 35.68 N/mm^2 in Gabal Hamza sample, the resistance values against chemical corrosion range from 0.03% in Gabal Hamza sample to 0.4% loss in weight in Arish sample, the linear shrinkage values during the firing process range from -0.46% in Sebaya sample to 9.16% in Heiz sample; the negative value means that the sample has been expanded.

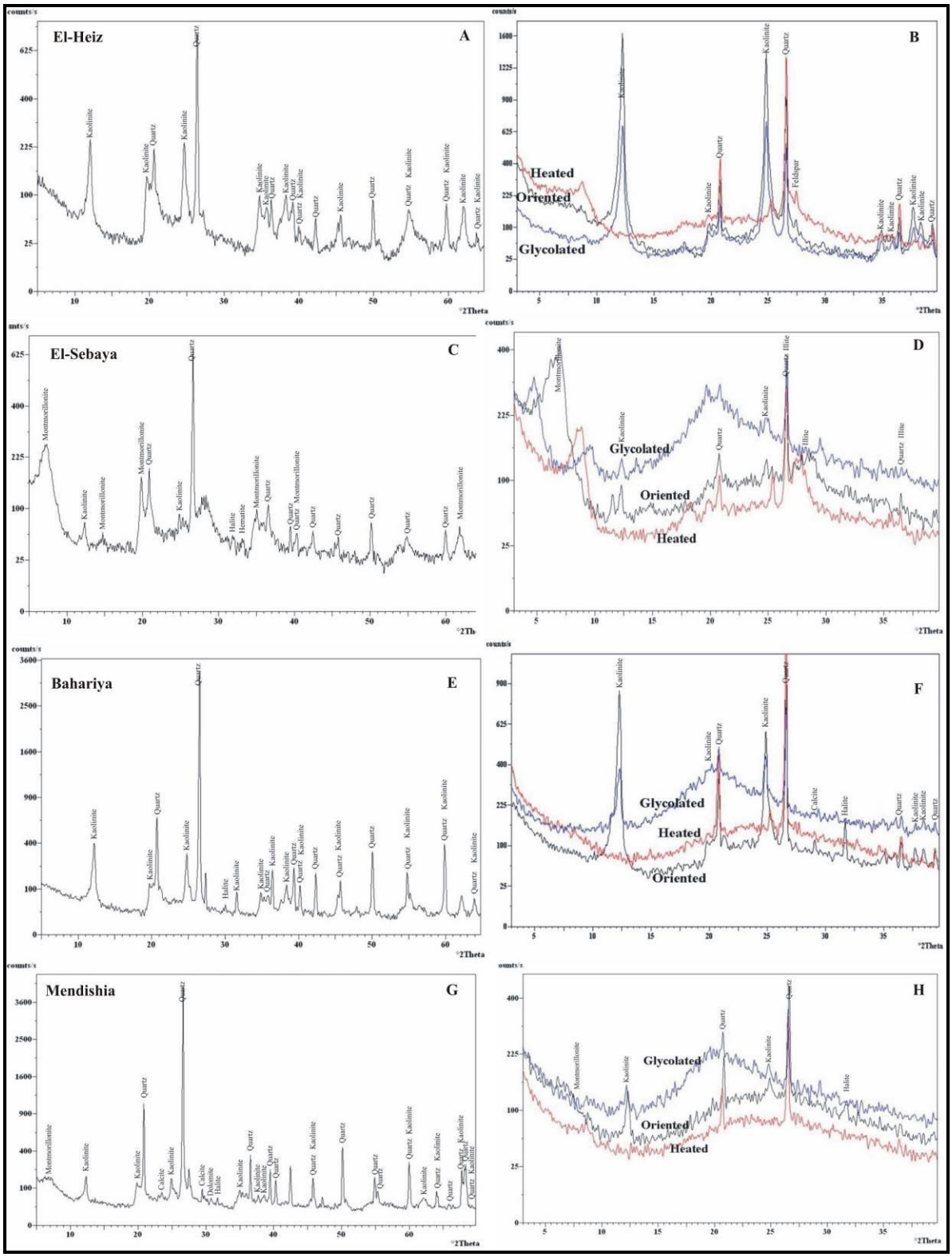

Fig.3. X-ray diffractions and X-ray diffractograms of the oriented specimen with different treatments. Runs shown are: Untreated, glycolate, and heated at ~550 °C for 2 hours.

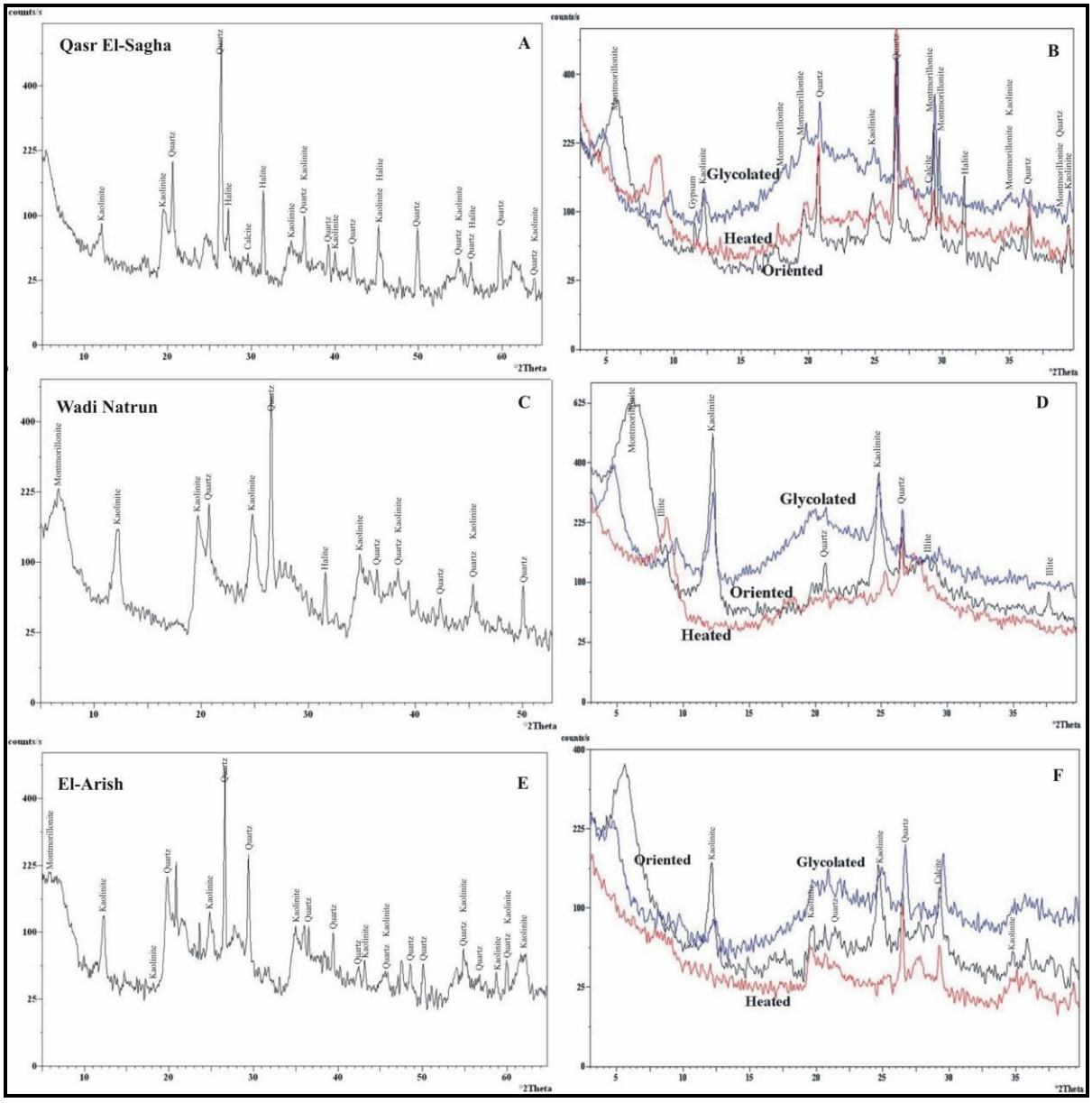

Fig.4. X-ray diffractions and X-ray diffractograms of the oriented specimen with different treatments. Runs shown are: Untreated, glycolate, and heated at ~550 °C for 2 hours.

The Pfefferkorn Test

The results of the Pfefferkorn test are shown in Figure (6). The Pfefferkorn test of the studied clay deposits show that the four studied clay samples (namely Monkar El-Wahsh 16%, Heiz 16.5%, Aswan 17 %, and Gabal Hamza 18% require a small quantity of water to be formed on the pressing machine. The other clay samples namely Bahariya, Qasr El-Sagha, Sebaya, Mendishia, Wadi Natrun, and Arish required a percentage higher than 18%.

Differential Thermal Analysis (DTA)

Thermal gravimetric analysis (TGA) and DTA thermograms are very important in all types of ceramic industry because the rate of firing is changed according to the points of decomposition and the points of loss in weight. Figures (7 and 8) show the differential thermal analysis (DTA) curves of the studied clay samples.

The low-temperature range in Bahariya (Fig. 7A), Heiz (Fig.7C), Monkar El-Wahsh (Fig. 8A), Mendishia (Fig. 8B), and Aswan (Fig. 8C) clays are characterized by one endothermic reaction peak occurs at the range of 69°-85.11°C and appears as a small symmetric peak. Meanwhile, an endothermic reaction peak occurs in the range of 103.72°-

109.55°C and appears as a small and broad peak in the Qasr El-Sagha (Fig. 7B), Wadi Natrun (Fig. 7D), Sebaya (Fig. 7E), Gabal Hamza (Fig. 7F) and Arish (Fig. 8D) clay samples.

Thermo-Gravimetric Analysis (TGA)

The obtained results are represented graphically as shown in Figures (9 and 10). The dehydration curves for the Aswan (Fig. 9A), Bahariya (Fig. 9C). Gabal considerable water loss below 600ºC. Meanwhile, a gradual loss from 500ºC to 700ºC is recorded in the Qasr El-Sagha (Fig. 9B), Arish (Fig. 9D), Mendishia (Fig. 9F), Wadi Natrun (Fig. 10B), and Sebaya (Fig. 10D) clay samples.

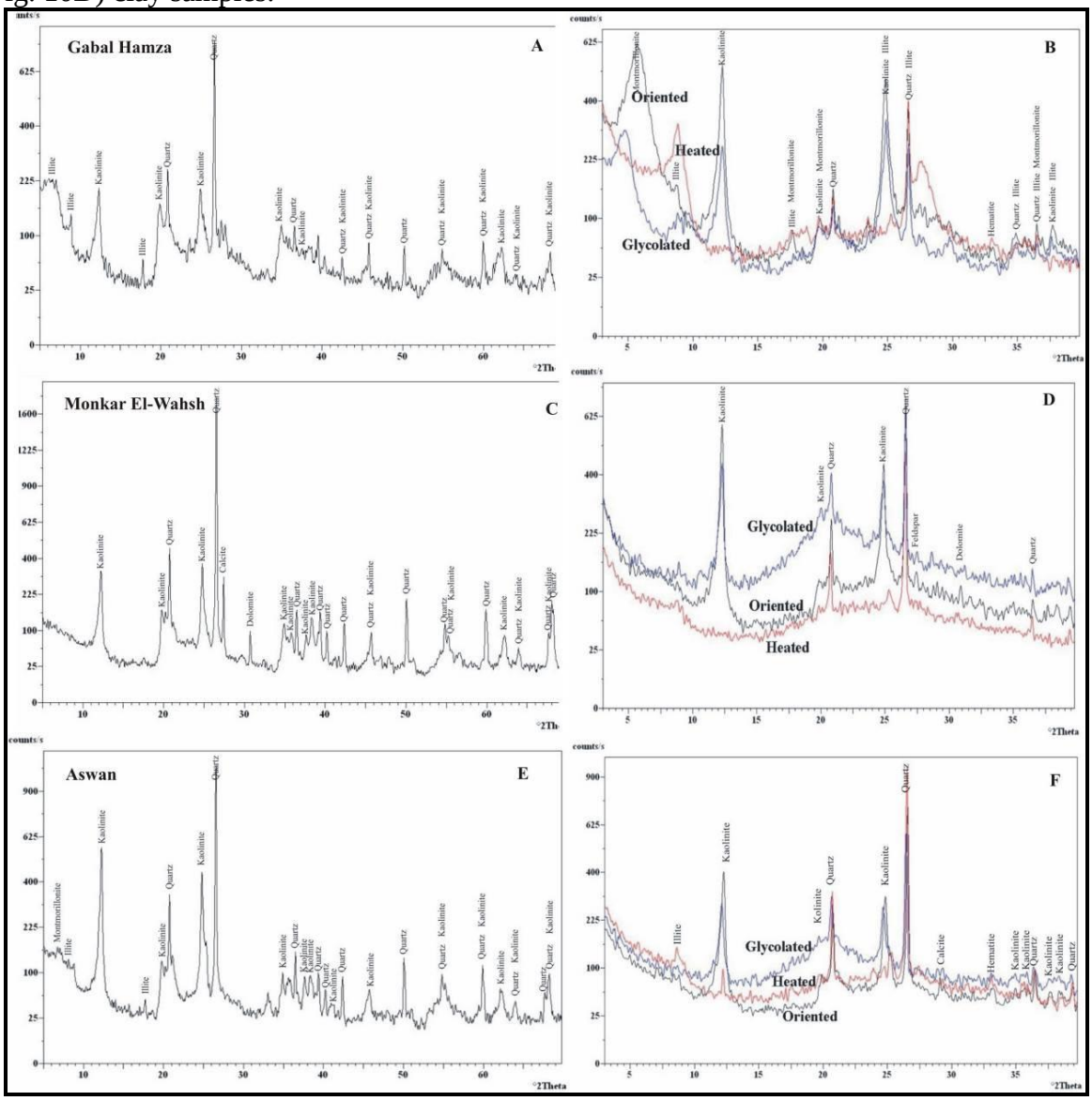

Fig.5. X-ray diffractions and X-ray diffractograms of the oriented specimen with different treatments. Runs shown are: Untreated, glycolate, and heated at ~550 °C for 2 hours.

Table 1. Geochemical data for major oxides (wt. %) of the studied composite clay samples.

Locality	SiO_2	Al_2O_3	TiO_2	Fe_2O_3	CaO	MgO	Na_2O	K_2O	P_2O_5	LOI	Total
Monkar El-Wahsh	59.8	17.9	0.2	5.5	2.5	2	0.95	0.26	0.9	9.8	99.81
Heiz	45.9	17.5	0.3	13.5	5	4	2	1.24	0.6	9.9	99.94
Bahariya	59.3	18.3	0.1	6.3	2.5	2	0.47	1.09	0.5	8.9	99.46
Qasr El-Sagha	55.6	16	0.3	9.5	3.3	2	1.36	0.9	0.2	10.5	99.66
Sebaya	56.7	14.2	0.4	12.7	3	2	1.72	1.04	0.4	7.8	99.96
Gabal Hamza	55.6	15.9	0.1	12.7	2.5	1.9	1.12	1.14	0.4	8.5	99.86
Mendishia	60.2	16.7	0.2	6	2.8	2	0.29	1.09	0.4	10.3	99.98
Wadi Natrun	57.3	11.5	0.1	12.7	2.5	2	0.9	1.62	0.3	11	99.92
Aswan	54.8	18.3	0.1	11.9	2.3	2.1	0.4	0.94	0.1	8.9	99.84
Arish	45.6	17.6	0.2	12.7	5	4.8	2.46	0.71	0.2	10.6	99.87
Average	55.08	16.39	0.20	10.35	3.14	2.48	1.17	1.00	0.4	9.62	99.83

Table 2. Geochemical data for trace elements (ppm) of the studied composite clay samples.

Locality	Cr	Ni	Cu	Zn	Zr	Rb	Y	Ba	Pb	Sr	Ga	V	Nb
Bahariya	119	20	36	27	838	32	84	5014	10	642	6	265	43
Qasr El-Sagha	115	32	30	80	474	73	51	3212	12	351	13	228	24
Heiz	166	34	46	57	420	86	44	5421	10	301	14	329	21
Wadi Natrun	164	47	34	65	347	58	36	4345	14	243	19	265	17
Sebaya	177	56	34	92	208	83	22	2915	10	105	7	273	10
Gabal Hamza	199	80	34	92	480	84	51	4925	15	318	13	337	24
Monkar El-Wahsh	159	35	47	54	530	102	56	5182	20	398	13	321	27
Mendishia	107	39	41	69	866	80	86	4978	10	641	14	238	44
Aswan	163	109	38	43	410	80	44	5345	4	269	--	359	21
Arish	112	64	37	73	421	74	49	3192	10	186	15	224	33
Average	148.1	51.6	37.7	65.2	499.4	75.2	52.3	4453	11.5	345.4	12.7	283.9	26.4

Table 3. Technical properties of the studied clay deposits compared with standard limits

Location	Fired Shrinkage %	Apparent porosity (%)	Water absorption (%)	Bulk density (gm/cm^3)	Dry M.O.R (n/mm^2)	Fired M.O.R (n/mm^2)	Chemical resistance	
							H_2SO_4	NaOH
Manufacturing limits	5 min.	20 max.	---	2 min.	1 min.	---	---	---
EN 295: 2013	---	---	6 max.	---	---	25 min.	Loss 0.25% max.	
Monkar El-Wahsh	7.40	7.02	2.93	2.39	1.22	32.96	0.04	0.07
Heiz	9.16	1.37	0.56	2.42	1.28	34.59	0.04	0.06
Gabal Hamza	9.08	3.19	1.28	2.49	2.33	35.68	0.05	0.03
Aswan	5.73	16.67	5.35	2.27	1.15	29.00	0.12	0.10
Mendishia	2.29	12.87	5.88	2.19	1.35	13.62	0.19	0.12
Bahariya	1.30	21.43	10.4	2.06	1.58	9.78	0.27	0.11
Wadi Natrun	6.03	5.00	1.62	2.00	2.45	31.29	0.31	0.15
Sebaya	-0.46	29.87	22.4	1.33	1.87	8.41	0.42	0.31
Qasr El-Sagha	Deformed	30.00	14.1	0.93	1.38	5.86	0.38	0.13
Arish	Deformed	36.72	42.9	0.86	1.47	4.36	0.40	0.32

Mineralogical Composition of the Fired Clay Samples

The mineralogical composition of the studied fired clay samples is shown in Figures (11 and 12). The results of the XRD patterns detected the phases in the various clay samples fired at 1200°C with a soaking time of 120 minutes. It is found that mullite, cristoballite, and quartz as major constituents, and hematite, and albite as minor phases.

Scanning Electron Microscope Investigation (SEM)

SEM photomicrographs of the studied clay specimens fired at 1200°C for 120 minutes soaking time with various magnification powers and its EDX spot microanalyses are shown in Figures (13 and 14).

Discussions

Mineralogical characterization

The studied clay deposits are composed mainly of SiO_2 and Al_2O_3 as major constitutes which reflect the mineralogical composition and classify the deposits as kaolinitic clay (Olusola et al. 2014).

Heiz, Gabal Hamza, Monkar El-Wahsh and Aswan clay deposits are composed mainly of kaolinite which is considered as the best mineral in the vitrified clay pipes manufacturing (Wahid, 2020).

Sodium-bearing minerals of the El-Sebaya clay deposits are non-plastic and reduce the green and dry strength of bodies (Kumari and Mohan, 2021).

El-Sebaya, Bahariya, Mendishia, Wadi Natrun, Al Arish and Qasr El-Sagha clay deposits are not suitable for the vitrified clay pipes industry because of the presence of halite and montmorillonite.

The percentages of the main oxides indicate the presence of smectite clay minerals in Arish, Aswan, Mendishia, Sebaya, and Wadi Natrun and therefore, the swelling potential of the samples is likely to be high. This result is confirmed by XRD analysis. The small percentage of CaO is probably to the presence of lime concentration in the limestone.

Glycolation removed the shoulder on the low-angle side of the illite peaks but in general, there is little evidence of expansion. The studied shale contains a small proportion of the illite component. Heating at ~550 °C did not provide a completely satisfactory distinction between kaolinite and chlorite (Brown and Brindley, 1980).

Heating for 1h did not entirely remove the kaolinite reflections and the montmorillonite reflection is reduced. The montmorillonite reflection remained for most, but not all, of the samples. However, there is a significant difference in basal spacings which permitted a distinction between the kaolinite and the montmorillonite in a few samples and the kaolinite and montmorillonite in most samples.

The main clay mineralogy of the shales is kaolinite. The diagenetic formation of kaolinite from the alteration of feldspars is one explanation and partial kaolinization of feldspars is observed. However, this needs not to be taken place during diagenesis and the geochemical evidence does not support major diagenetic kaolinization. The more likely explanation is that the difference is a depositional one. Kaolinite is known to be concentrated in many near-shore sediments and to decrease in abundance with distance from the shoreline as other clay minerals increase (Parham, 1966).

Many types of clay and shale are often contaminated with accessory minerals inherited from the parent rocks or formed during deposition and diagenesis. Small percentages of such accessory minerals will influence the vitrified clay pipe properties, sometimes quite disproportionate to their amount. The presence of titanium minerals even in low percentages (TiO_2 > 1%) will produce an ivory ceramic tint on firing. Moreover, the presence of calcite and dolomite (Monkar El-Wahsh shale) as well as feldspars and alkali-bearing minerals will affect, to a large extent, the vitrification temperature and porosity.

Geochemical characterization

The chemical composition of the clay deposits under consideration is compared with published average clay deposits (2, Table 4) and regional average clay deposits composition (3 to 7, Table 4). The studied clay deposits resemble those of the Gabal Ghorabi clay deposits of Abdou and Shehata (2007), average clay deposits of Pettijohn (1957), and average clay deposits of Turekian and Wedepohl (1961). The only apparent discrepancy as can be noted in Table (4) lies in the SiO_2 and Al_2O_3 contents. There is also a great chemical similarity between the analyzed clay deposits and some published average clay deposits and regional average clay deposits (Table 4).

The frequencies of most elements show discordance when compared with the published data by NASC (North-American shale composite; Gromet *et al.,* 1984), Bida clay deposits (Okunlola and Idowu, 2012), and PAAS (Post Achaean Australian Average Shale; Taylor and McLennan, 1985) as seen in Table (4). These discrepancies may be attributed to different factors such as source rock composition, and sedimentological and diagenetic conditions.

SiO_2 may occur as quartz disseminated with kaolinite or deposited with the tiny flakes of the clay minerals (Bain and Smith 1987; Moore and Reynolds 1997).

High alumina (Al_2O_3) content is recorded in the argillaceous and clayey sediments. The average content of alumina in the studied clay deposits of the different localities (16.39%) is similar to that of the average clay deposits of Pettijohn (1975) and NASC (15.40% and 17.05 % respectively, Table 4), slightly higher than that of the average Bida clay deposits (16.88%) of Okunlola and Idowu (2012) but much higher than the argillaceous sediments of PAAS (Taylor and McLennan, 1985).

The Al_2O_3 concentration is thought to be a good measure of detrital influx. Generally, the studied clay deposits show coherence between silica and alumina indicating that both molecules are carried mainly in the clay minerals.

The average content of Fe_2O_3 in the studied clay deposits samples is 10.35 %. The recorded average is higher than those of average clay deposits of Gabal Ghorabi 4.80 %,

average clay deposits of Pettijohn (1975), average clay deposits of Turekian and Wedepohl (1961), Bida clay deposits, PAAS clay deposits, and NASC clay deposits (4.80%, 4.02%, 4.72 %, 3.75%, 7.18 %, and 5.70 % respectively).

Iron is present either in the structure of clay minerals and/or as an independent Fe-mineral such as goethite, hematite, and limonite. Sharma (1979) stated that in the marine environment, the hydroxides of iron are carried as particles and colloids in suspension and therefore, tend to aggregate in the fine fraction of sediments. The enrichment of Fe_2O_3 in the studied clay deposits may be attributed to their formation under more reducing conditions with a high input of non-reactive iron to the basin. There is a strong positive correlation between Fe_2O_3 and the TiO_2, CaO, MgO, Na_2O, K_2O, Cr, Ni, Zn, Rb, V (r = 0.16, 0.42, 0.43, 0.60, 0.46, 0.53, 0.53, 0.44, 0.12 and 0.22 respectively, Table 5) and negative correlation between Fe_2O_3 and SiO_2, Al_2O_3, P_2O_5, Cu, Zr, Y, Ba, Pb, Sr, Nb (r = -0.68, -0.39, -0.48, -0.30, -0.80, -0.79, -0.29, -0.31, -0.83 and -0.70 respectively). This may be due to the association of Fe^{3+} with clay minerals.

The mean value of Na_2O (1.17%) is rather similar to that of average clay deposits of PAAS, NASC, Pettijohn (1975) and Turekian and Wedepohl (1961) clay deposits (1.19%, 1.13%, 1.30%, and 1.30% respectively) and lower than those of average clay deposits of Bida clays (0.06%), while it is higher than those of Gabal Ghorabi clay deposits (3.00%). Na_2O shows a negative correlation with SiO_2 and Al_2O_3 (-0.81 and -0.06 Table 5). This may be due to the presence of Na_2O in the form of water-soluble salts (mainly halite). Halite is detected by XRD analysis in some of the studied clay deposit samples.

The average content of potassium (K_2O) in the studied clay deposits (1.00 %) is lower than those of the average clay deposits of NASC, Pettijohn (1975), Turekian and Wedepohl (1961), and PAAS clay deposits (3.97%, 3.24%, 3.10%, and 3.68% respectively). This may be due to the enrichment of clays in those clay deposits mixed-layers, different from the studied clay deposits, where smectite clays dominate. The mean value of K_2O is similar to that of average clay deposits of Gabal Ghorabi and Bida clay deposits (1.10% and 1.39 %). K_2O shows a negative correlation with SiO_2, Al_2O_3, TiO_2, CaO, MgO, Na_2O, P_2O_5, Cu, Zr, Rb, Y, Pb, Sr, V and Nb (r = -0.04, -0.62, -0.17, -0.05, -0.11, -0.12, -0.38, -0.39, -0.09, -0.49, -0.14, -0.31, -0.04 and -0.20 respectively, Table 5). This indicates that the K_2O is not associated with aluminosilicate phases.

The K_2O content is in agreement with the results of the clay mineral investigations because the low content reflects the absence of or the low content of illite minerals.

The weak positive correlation of K_2O with Fe_2O_3, Ba, Cr, and Zn (r =0.46, 0.05, 0.21, and 0.08 respectively) in samples with less illite content can be interpreted that potassium is preferentially adsorbed by clays (Millot, 1970).

In the studied clay deposits, vanadium attains an average concentration of 283.9 ppm and varies from 224 ppm to 359 ppm. The average vanadium content in the studied clay deposits is higher than those of average clay deposits (130 ppm) of Turekian and Wedepohl (1961) and also higher than vanadium in average clay deposits of NASC (130 ppm), Bida (108.77 ppm) and PAAS (150 ppm). It is suggested that some vanadium may be complex within the kerogen molecule (Dechaine, 2010). The high concentrations of vanadium in the inorganic fraction may be the result of oxidation and weathering of the organic matter and the subsequent mobilization and concentration in host rocks (Riley and Saxby, 1983). Vanadium shows a positive correlation with some of the other trace elements, such as Ba, Rb, Cu, Ni, and Cr (r=0.68, 0.40, 0.42, 0.51, and 0.77, Table 5).

The average chromium content of the studied clay deposits is 148.1 ppm. This is higher than the Cr content in average clay deposits (90 ppm) of Turekian and Wedepohl (1961) and also higher than Cr in average clay deposits (55 ppm) of Gabal Ghorabi and average clay deposits (125 ppm) of NASC. Chromium shows a positive correlation with Fe_2O_3 (0.53), K_2O

(0.21), and P_2O_5 (0.21). However, Cr may be adsorbed on iron and manganese oxides, clays, apatite, and organic matter (Prevot, 1990).

Table 4. Comparison of the chemical composition of the studied clay deposits with published average clay deposits (1 to 2) and regional average composition (3 to 7).

Oxides	1	2	3	4	5	6	7
SiO_2	55.08	54.00	64.82	58.10	58.50	61.26	62.40
Al_2O_3	16.39	13.40	17.05	15.40	15.00	16.88	18.78
TiO_2	0.20	1.60	0.80	0.60	0.77	1.74	0.99
Fe_2O_3	10.35	4.80	5.70	4.02	4.72	3.75	7.18
MgO	2.48	1.20	2.83	2.40	2.50	0.16	2.19
CaO	3.14	2.00	3.51	3.10	3.10	0.05	1.29
Na_2O	1.17	3.00	1.13	1.30	1.30	0.06	1.19
K_2O	1.00	1.10	3.97	3.24	3.10	1.39	3.68
P_2O_5	0.4	0.00	0.15	0.20	0.16	0.08	0.16
Trace elements (ppm)							
Sr	345	178	142	--	300	59	200
Ba	4453	245	636	--	580	394	650
V	283	407	130	--	130	108	150
Ni	51	19	58	--	68	19	55
Cr	148	55	125	--	90	--	--
Zn	65	471	--	--	95	116	85
Cu	37	52	--	--	45	14	50
Zr	499	710	200	--	160	1156	210

1. Average of the studied clay deposits.
2. Clay deposits from Gabal Ghorabi Member (Abdou and Shehata, 2007).
3. NASC (North-American shale composite; Gromet et al., 1984).
4. Average clay deposits (Pettijohn, 1957).
5. Average clay deposits (Turekian and Wedepohl, 1961).
6. Bida clay deposits (Okunlola and Idowu, 2012).
7. PAAS (Post Achaean Australian Average Shale; Taylor and McLennan, 1985).

Table 5. Pearson's correlation coefficient values of each pair of elements of the studied clay deposits.

	SiO_2	Al_2O_3	TiO_2	Fe_2O_3	CaO	MgO	Na_2O	K_2O	P_2O_5	Cr	Ni	Cu	Zn	Zr	Rb	Y	Ba	Pb	Sr	V	Nb
SiO_2	1.00																				
Al_2O_3	-0.20	1.00																			
TiO_2	-0.24	-0.10	1.00																		
Fe_2O_3	-0.68	-0.39	0.16	1.00																	
CaO	-0.91	0.21	0.46	0.42	1.00																
MgO	-0.92	0.29	0.20	0.43	0.94	1.00															
Na_2O	-0.81	-0.06	0.57	0.60	0.85	0.78	1.00														
K_2O	-0.04	-0.62	-0.17	0.46	-0.05	-0.11	-0.12	1.00													
P_2O_5	0.24	0.21	0.14	-0.48	-0.05	-0.09	-0.03	-0.38	1.00												
Cr	-0.01	-0.32	-0.03	0.53	-0.25	-0.23	0.07	0.21	0.21	1.00											
Ni	-0.20	0.04	-0.31	0.53	-0.17	0.01	-0.04	0.00	-0.55	0.45	1.00										
Cu	-0.14	0.49	0.04	-0.30	0.24	0.30	-0.01	-0.39	0.71	0.06	-0.18	1.00									
Zn	-0.12	-0.52	0.48	0.44	0.16	0.00	0.46	0.08	-0.21	0.29	0.18	-0.41	1.00								
Zr	0.42	0.47	-0.39	-0.80	-0.23	-0.20	-0.59	-0.09	0.23	-0.60	-0.43	0.22	-0.48	1.00							
Rb	-0.16	0.12	0.40	0.12	0.15	0.10	0.26	-0.49	0.31	0.39	0.30	0.48	0.45	-0.37	1.00						
Y	0.37	0.51	-0.41	-0.79	-0.18	-0.15	-0.55	-0.14	0.21	-0.63	-0.41	0.22	-0.48	1.00	-0.36	1.00					
Ba	0.18	0.41	-0.56	-0.29	-0.28	-0.17	-0.57	0.05	0.42	0.23	0.06	0.64	-0.61	0.46	0.07	0.44	1.00				
Pb	0.31	-0.24	-0.03	-0.31	-0.18	-0.21	0.06	-0.31	0.69	0.22	-0.42	0.21	0.23	0.01	0.30	0.02	0.04	1.00			
Sr	0.52	0.41	-0.36	-0.83	-0.32	-0.33	-0.67	-0.04	0.30	-0.52	-0.50	0.23	-0.52	0.98	-0.37	0.96	0.52	0.07	1.00		
V	-0.03	0.25	-0.27	0.22	-0.26	-0.17	-0.21	-0.06	0.28	0.77	0.51	0.42	-0.23	-0.24	0.40	-0.25	0.68	0.00	-0.16	1.00	
Nb	0.20	0.54	-0.39	-0.70	-0.01	0.07	-0.37	-0.20	0.12	-0.73	-0.36	0.20	-0.44	0.94	-0.38	0.96	0.30	-0.04	0.86	-0.37	1.00

Chromium is presumably derived from a source dominated by mafic volcanic rocks (Gill, 1981). High Cr and Ni concentrations and the positive correlation between the two elements have been used as an indicator of mafic and ultramafic provenance for the sedimentary origin. The concentration of Cr and Ni in clay deposits further reflects the incorporation of Cr and Ni ions into clay particles during the weathering of ultramafic rocks containing chromite and other Cr and Ni-bearing minerals (Garver *et al.*, 1994). The enrichment in Cr and Ni in the studied clay deposits may indicate that mafic to ultramafic components were among the basement complex, from which the sediments were derived.

Strontium is abundant in the studied clay deposits samples. It ranges between 105 ppm and 642 ppm with an average of 345.4 ppm. This average is higher than the Sr content in the average clay deposits (300 ppm) of Turekian and Wedepohl (1961), (200 ppm) of PAAS and also higher than Sr in average clay deposits (178 ppm) of Gabal Ghorabi and average clay deposits (142 ppm) of NASC. Sr may be concentrated by non-calcareous plankton (Knauer

and Martin, 1973) and especially aragonitic materials and shells, as well as by primary apatite in the bones and teeth of vertebrates. In the present study, except for clay deposits of (105 ppm) Sebaya, (186 ppm) Arish, (243 ppm) Wadi Natrun and (269 ppm) Aswan, the studied clay deposits show high strontium values. This is related to the association of Sr with CaO and organic matter.

Zirconium in the studied clay deposits samples shows an average of 499.9 ppm. This average is lower than the zirconium content in the average clay deposits (710 ppm) of Gabal Ghorabi and (1156.54 ppm) of Bida and also higher than Zr in the average clay deposits (160 ppm) of Turekian and Wedepohl (1961), (200 ppm) of NASC and (210 ppm) of PAAS. It shows high values in Bahariya and Mendishia clay deposits samples (838 ppm and 866 ppm respectively). This indicates that Zr may be incorporated into organic matter or adsorbed by clay minerals. Zirconium shows positive correlation with SiO_2 Al_2O_3, Y, Ba, Sr and Nb (r=0.42, 0.47, 1.00, 0.46, 0.98 and 0.94 respectively). This is the result of the close association between these elements and clays and therefore reflects their terrigenous origin.

Physical properties of the clay deposits

The Pfefferkorn Test

The plasticity test of the studied clay deposits shows that the samples of Monkar El-Wahsh, Heiz, Aswan, and Gabal Hamza need less than 18% of water during extruding process which consider them suitable for clay pipes industry. On the other hand, Bahariya, Qasr El-Sagha, Sebaya, Mendishia, Wadi Natrun, and Arish required a percentage higher than 18% that causes problems of deformation, cracks and high consumption of thermal energy. Generally, deformation heights for bodies to be extruded lie between ~25 mm for soft extrusion and ~37 mm for stiff extrusion (Händle, 2007).

Differential Thermal Analysis (DTA)

According to Grim (1968), the small endothermic peak at about 100°C in Bahariya (Fig.10A), Heiz (Fig.10C), Monkar El-Wahsh (Fig.11A), Mendishia (Fig.11B), and Aswan (Fig.11C) clay samples is attributed to the dehydration of disordered kaolinite mineral. According to El-Askary (1972) and Grim (1968), the endothermic peak of the studied clay is related to the dehydration of disordered kaolinite.

According to Grim (1951) and Grim (1968), the second large endothermic reaction peak represents the loss of the interlayer water of both montmorillonite and illite structures. Also, the small endothermic peak at 283°- 333.2°C is related to the dehydration of goethite [FeO(OH)] mineral associated with the clay deposits, especially Sebaya and Aswan samples.

In the range between 400°-700°C, there are large symmetric endothermic reaction peaks at 545.95°C, 544.37°C, 539.33°C, 541.31°C, 543.27°C, 534.81°C, 534.77°C, 526.66°C, 541.24°C, and 534.97°C, characterizing Bahariya, Qasr El-Sagha, Heiz, Wadi Natrun, Sebaya, Gabal Hamza, Monkar El-Wahsh, Mendishia, Aswan and Arish clay samples, respectively. These peaks are caused by the loss of the structural (OH), from montmorillonite, illite, and kaolinite lattices (Grim and Bradley, 1940). Hunziker (1966) stated that the sedimentary micas (illites) lose their $(OH)^-$, which has been part of the octahedral layers between 500°-650°C.

According to Grim (1968), the relatively low temperature at which montmorillonite peaks take place may indicate that the montmorillonite mineral of the analyzed sample is rich in iron.

At a high-temperature range (700°-1000°C) all studied clay samples have only a sharp exothermic reaction peak that takes place at 940°-968.33°C without any weight 1oss. Ekosse (2001) recorded that the mullitization peak temperature is at 975°C in appreciable amounts by heating the well-crystallized kaolinite. A somewhat variation in the temperature may be due to the effect of impurities, even in very small amounts. The content of mullite depends on the crystallinity of kaolin and the firing temperature (Chavez and Johns, 1995).

Thermo-Gravimetric Analysis (TGA)

From the TGA-DTA thermograms, the TGA curves show the decomposition of the samples ranging from 100% to 89%, which corresponds to a loss of weight ranging from 11 gm to 7.8 gm (9.4% of the total weight). This is ideal for kaolinite because an ideal loss in weight of pure kaolinite is 14% (Newman, 1987).

The difference in the experimental loss in weight compared to the ideal in the literature is because the analyzed clay deposits are not solely kaolinite but contain montmorillonite, illite, quartz, calcite, halite, and dolomite as revealed by chemical and mineralogical analyses.

Physical properties of the clay deposits after thermal treatment

Mineralogical Composition of the Fired Clay Samples

In the different fired specimens, the detected minerals by the XRD analysis are mullite, cristoballite, and quartz as major constituents and hematite, and albite as a minor constituent in all tested fired specimens. The studied clay samples produced a high amount of mullite that gives high values in crushing strength and are preferable to be used in the vitrified clay pipes industry.

The most important mineral in the heavy structural ceramic industry is the mullite which generate during the thermal treatment of clay minerals especially the kaolinite higher than 1000°C (Anggono, 2005). Therefore, Gabal Hamza, Heiz, Monkar El-Wahsh and Aswan deposits are suitable for clay pipes industry.

Physical properties

These results of water absorption show that the studied clay samples are well matched with the international standard limit of water absorption (6%) according to ES-56:2005, EN-295:2013, and ZP WN 295: 2016.

The water absorption percent of the studied clay deposits reflects the behavior of bulk density and apparent porosity. There is a reverse relationship between water absorption and bulk density and positive relationship between water absorption and apparent porosity (Fig. 15). According to the international standards EN 295-1, 2013 and ZP WN 295, 2016, the maximum accepted limit of water absorption is 6%. Therefore Heiz, Monkar El Wahsh, Gabal Hamza, Aswan and Mendishia matched the standard requirements. The maximum accepted limit of apparent porosity is 20% according to the manufacturing limits, the minimum accepted limit for bulk density is 2 gm/cm^3. Therefore, Bahariya, Sebaya, Qasr El Sagha and Arish clay deposits are excluded from the application of clay pipe industry.

There is also a negative relationship between the mechanical strength (MOR) and chemical resistance; higher MOR means lower chemical resistance (Fig. 16).

According to the international standard EN 295: 2013; the maximum accepted limit for the chemical resistance is 0.25% and the minimum value of MOR is 25 n/mm^2. Therefore, Bahariya, Wadi Natrun, Sebaya and Arish clay deposits are excluded from the application of clay pipes industry. There is a positive relationship between MOR and shrinkage; higher MOR means higher shrinkage (Fig. 16).

According to the manufacturing limits, the minimum accepted shrinkage percent is 5% so, Sebaya, Mindishia and Bahariya clay deposits will be excluded from the clay pipes application.

Scanning Electron Microscope Investigation (SEM)

The SEM photomicrographs of produced fired Heiz, Monkar El-Wahsh, Gabal Hamza and Aswan clay samples show very fine cemented fragments of different phases. This is due to the high quality of these products whether in water absorption, resistance to crushing strength, or increase in bulk density. Consequently, the clay deposits of these localities produce fired products of the first-grade of quality.

The photomicrographs also show coarse cemented fragments, this is expected due to the medium quality of these samples whether in water absorption and resistance to crushing strength. These phases are present in samples of Bahariya and Mendishia clay deposits and aforementioned these clay deposits are considered second grade and can be used in a blend with samples of high-quality fine cemented texture in the production of vitrified clay pipes.

The photomicrographs show holes due to bubbles formation; it could be an evidence of bloating phenomena. These phenomena may cause a decrease in the resistance to crushing strength and bulk density and also increasing in water absorption and apparent porosity. These phases are present in samples of Wadi Natrun, Arish, Qasr El-Sagha, and Sebaya shales which of these clay deposits cannot use in the production of vitrified clay pipes.

Therefore, the studied deposits can be classified into three grades:

1. The first grade shows a very fine cemented texture of different phases. This is expected due to the high quality of these specimens supported by the result of water absorption, resistance to crushing strength, and bulk density properties. These grades are present in Heiz (Fig.13A), Aswan (Fig.13B), Gabal Hamza (Fig.13C), and Monkar El-Wahsh (Fig.13D) clay deposits.

2. The second grade shows coarse cemented fragments. This is expected due to the medium quality of these clay samples whether in water absorption or resistance to crushing strength. These grades are present in the clay deposits of Bahariya (Fig.13E) and Mendishia (Fig.13F).

3. The third-grade shows holes form due to bubbles formation; it could be evident to bloating phenomena. These results are due to a decrease in the resistance to crushing strength and bulk density and also an increase in water absorption and apparent porosity. This grade is present in the Wadi Natrun (Fig.14A), Arish (Fig.14B), Qasr El-Sagha (Fig.14C), and Sebaya (Fig.14D) clay deposits.

Conclusions

The mineralogical, geochemical, and technological characteristics of some Egyptian clay deposits to verify their properties for the vitrified clay pipes (VCP) industry are compared to Sweillem Vitrified Clay Pipes Company (SVCP) standard and international standards.

According to the applicable standards of SVCP Company of the weight percentages of the main oxides of clay deposits are suitable for the production of vitrified clay pipes and their accessories. Only the Monkar El-Wahsh, Heiz, Aswan and Gabal Hamza clay samples are suitable for this purpose. The other samples are not confirmed for the VCP industry but may be used partly when mixed with the high-quality clay deposits.

The XRD of the studied clay samples show that all samples consist of kaolinite and quartz as major minerals constituents. Some of these clay samples contain large proportions of montmorillonite which is not preferred to be used in the VCP industry as needs a large amount of water in the mixing.

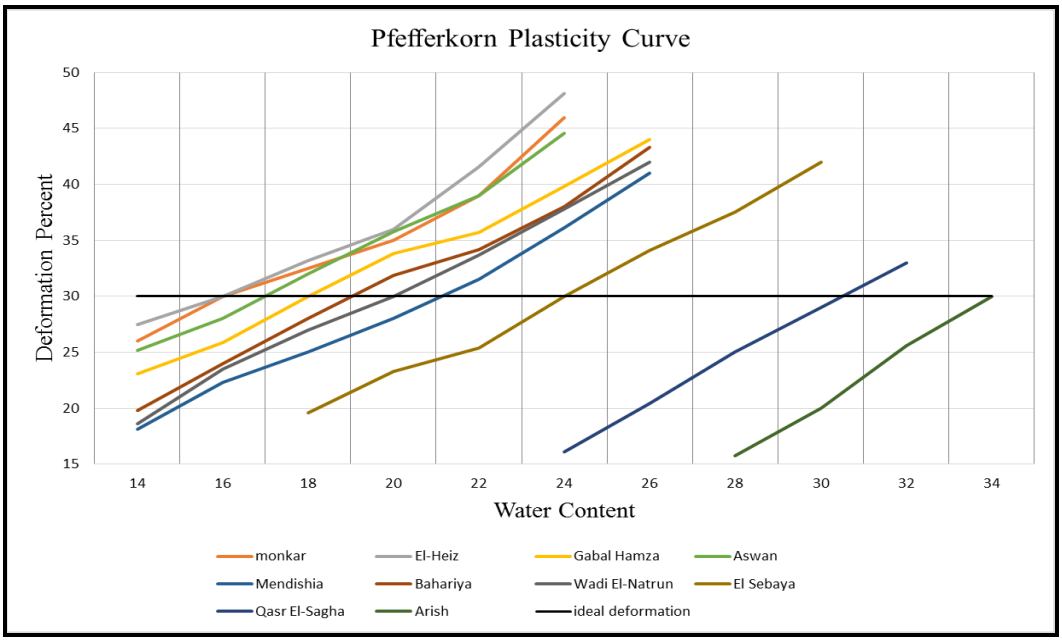

Fig.6. The Pfefferkorn plasticity curve.

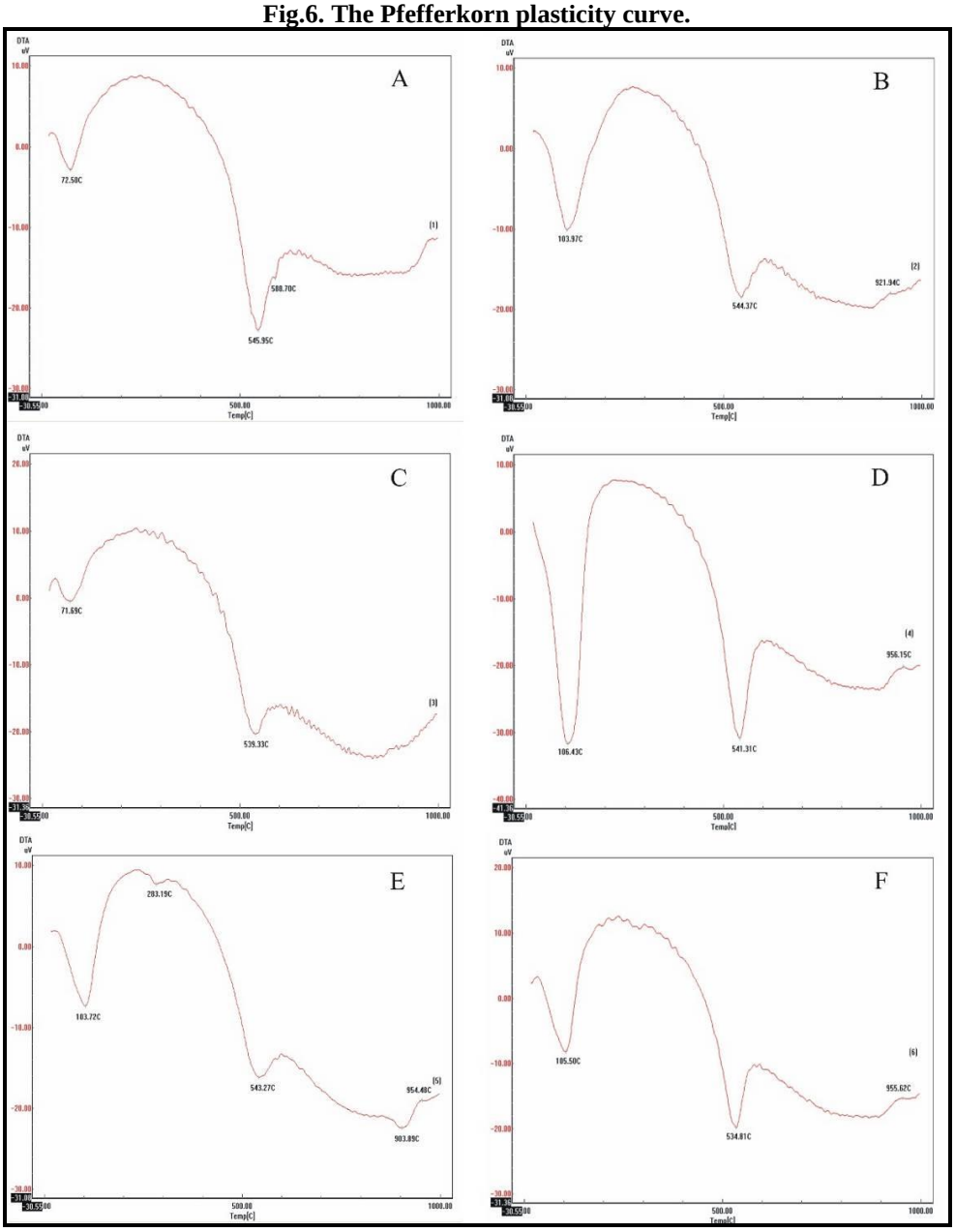

Fig.7. DTA pattern of the studied clay samples.

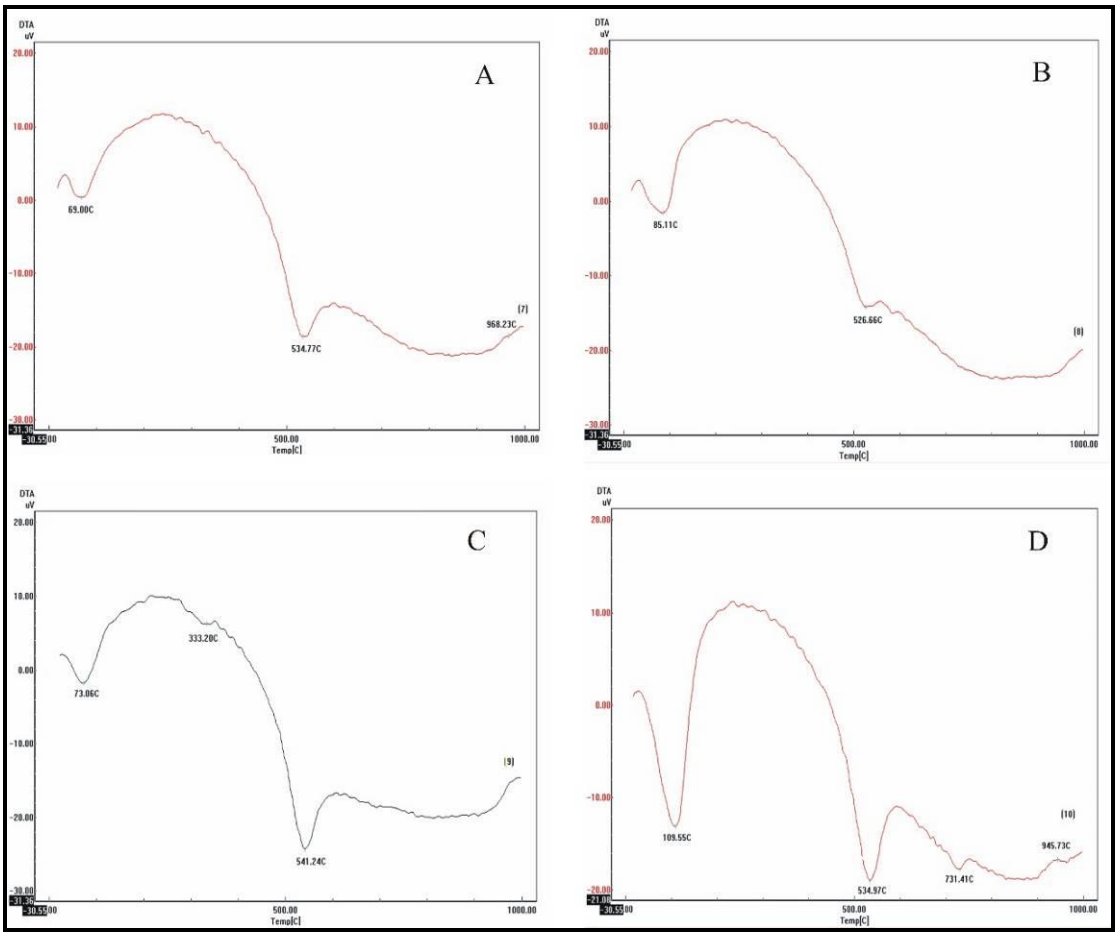

Fig.8. DTA pattern of the studied clay samples.

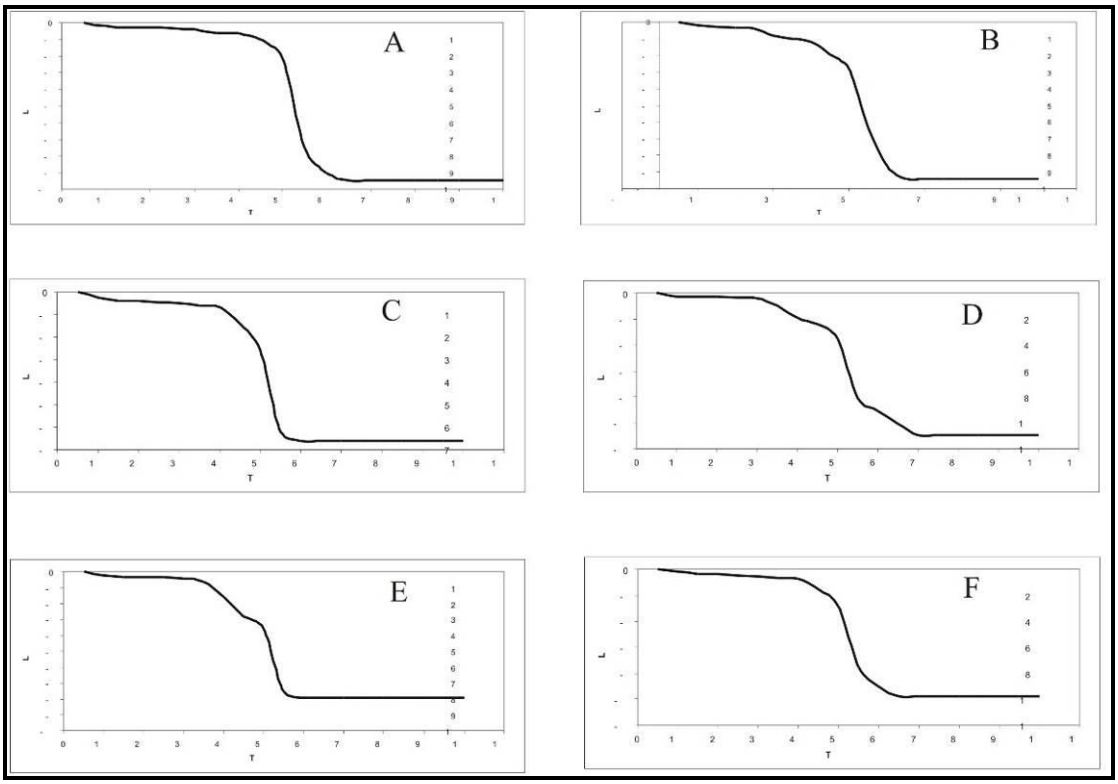

Fig.9. Weight-loss curve for TGA pattern of the studied clay samples.

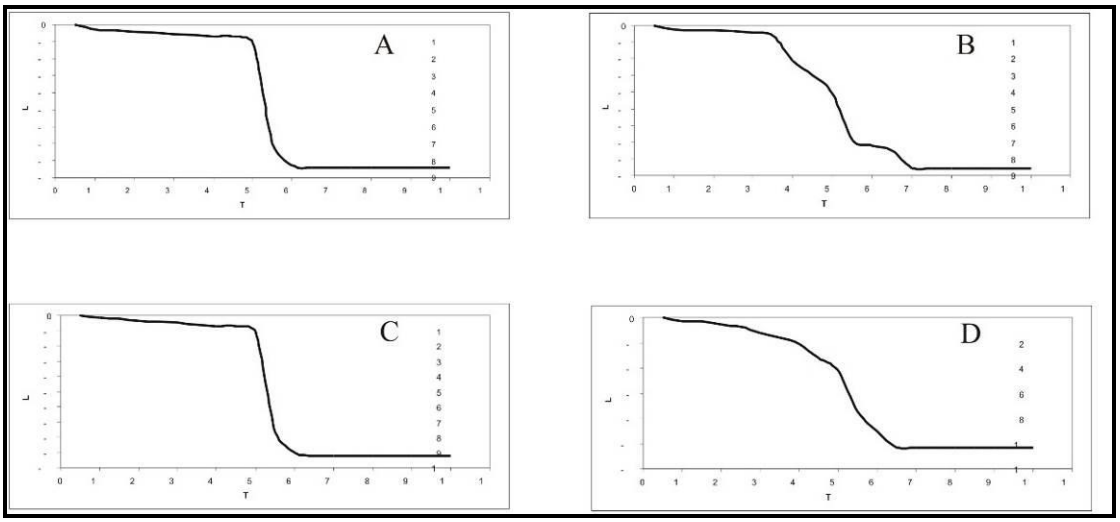

Fig.10. Weight-loss curve for TGA pattern of the studied clay samples.

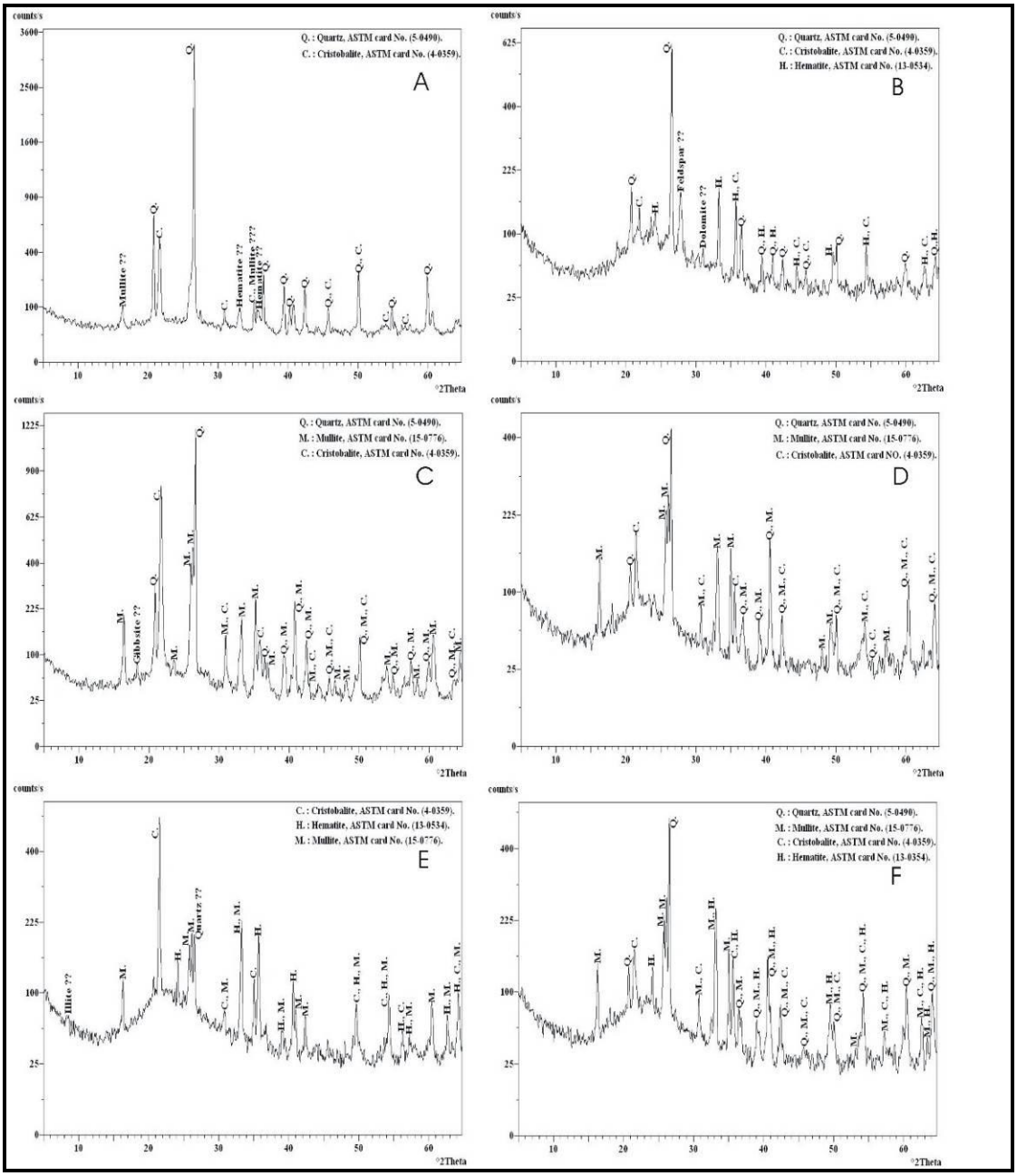

Fig.11. X-ray diffraction pattern of the fired clay samples.

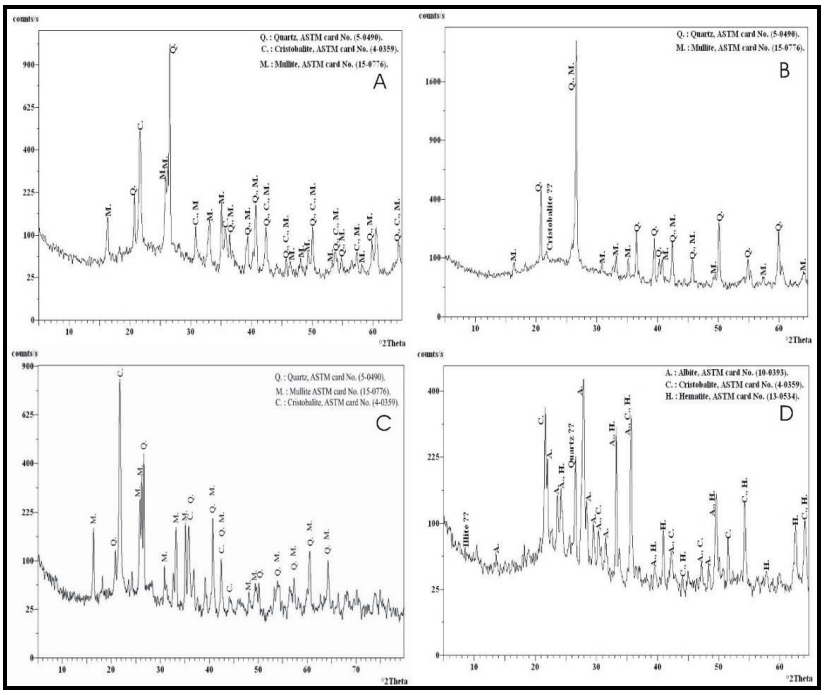

Fig.12. X-ray diffraction pattern of the fired clay samples.

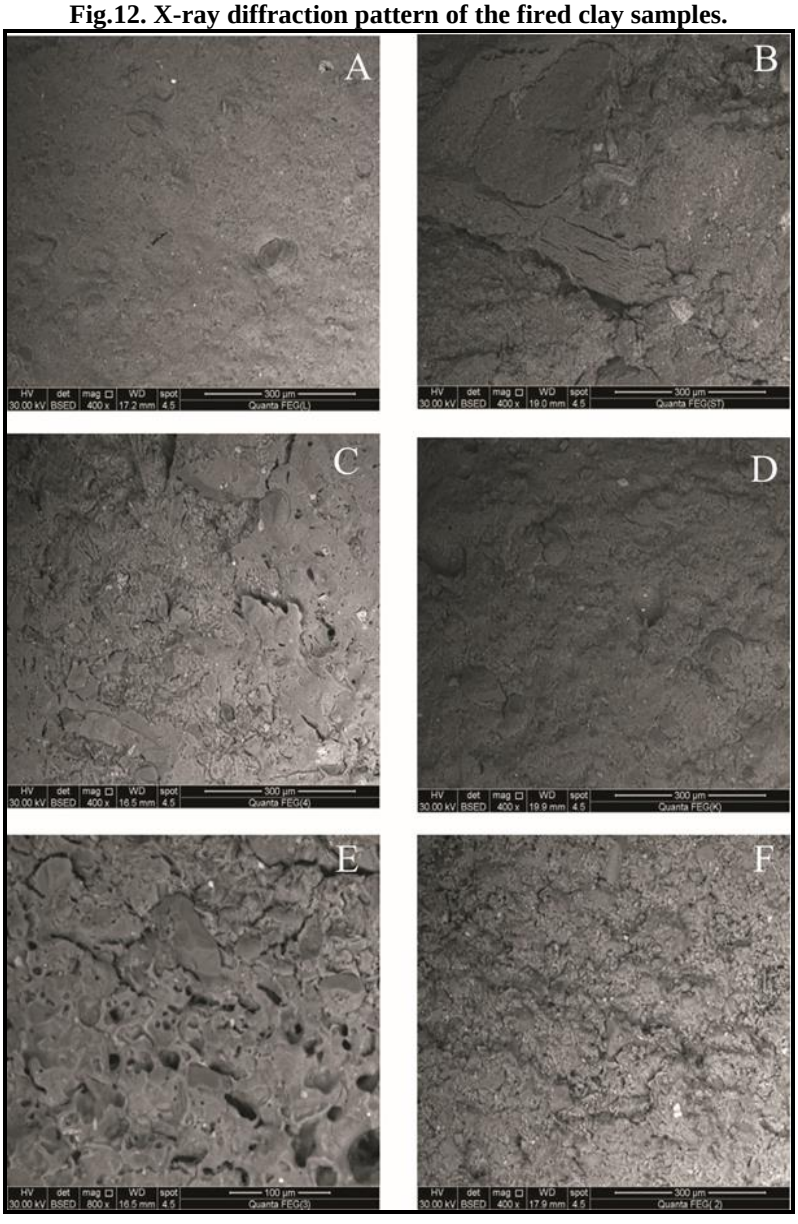

Fig.13. Close-up view of SEM photomicrograph showing clay samples fired at 1200°C

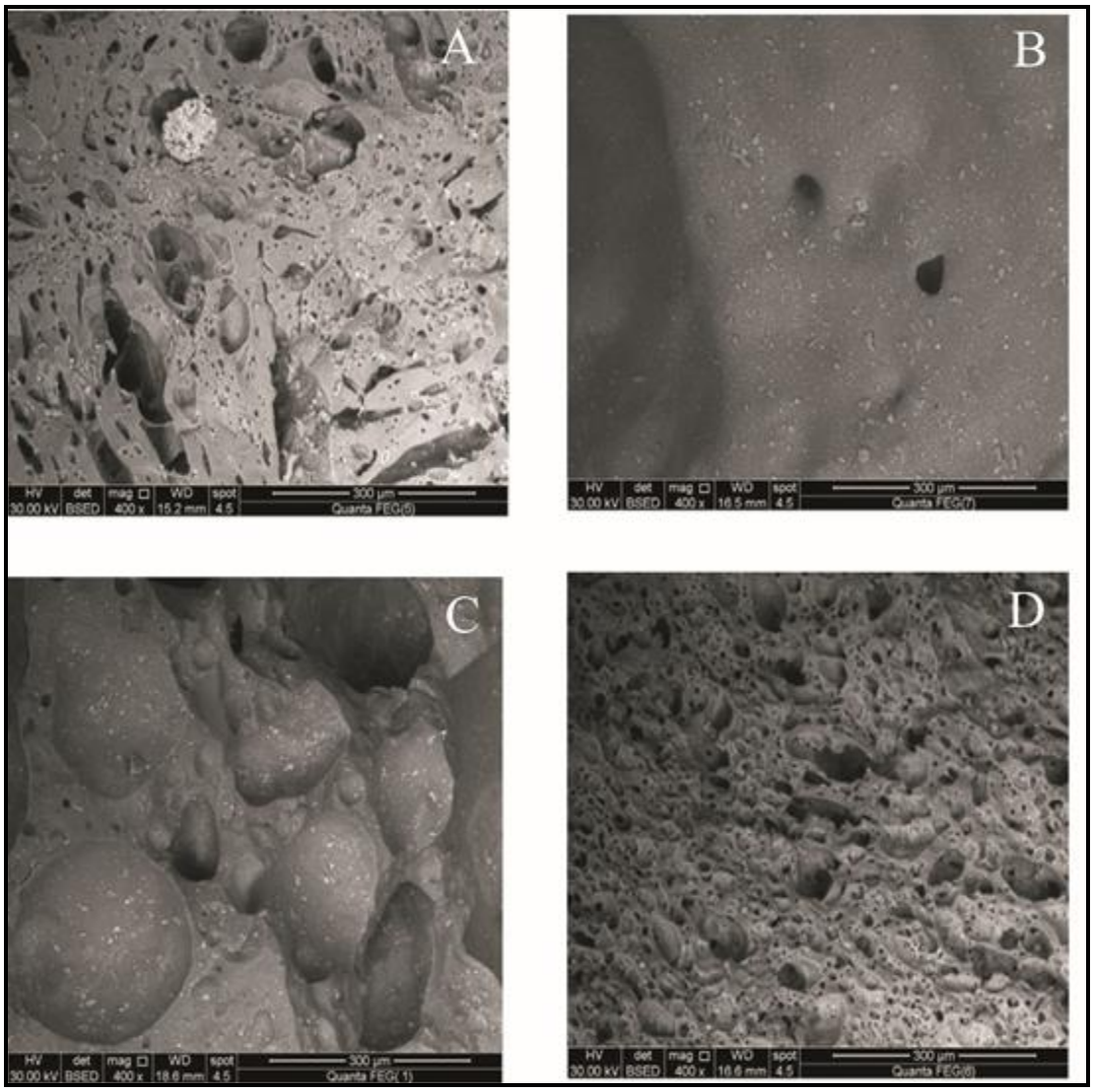

Fig.14. Close-up view of SEM photomicrograph showing clay samples fired at 1200°C.

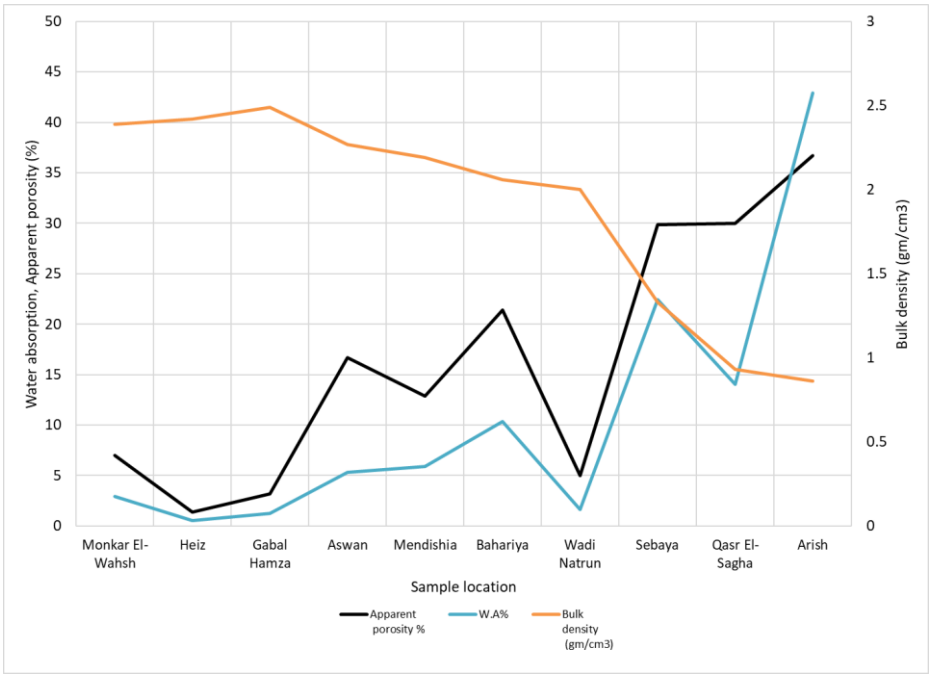

Fig.15. The relationship between the studied clay samples vs water absorption, bulk density, and apparent porosity.

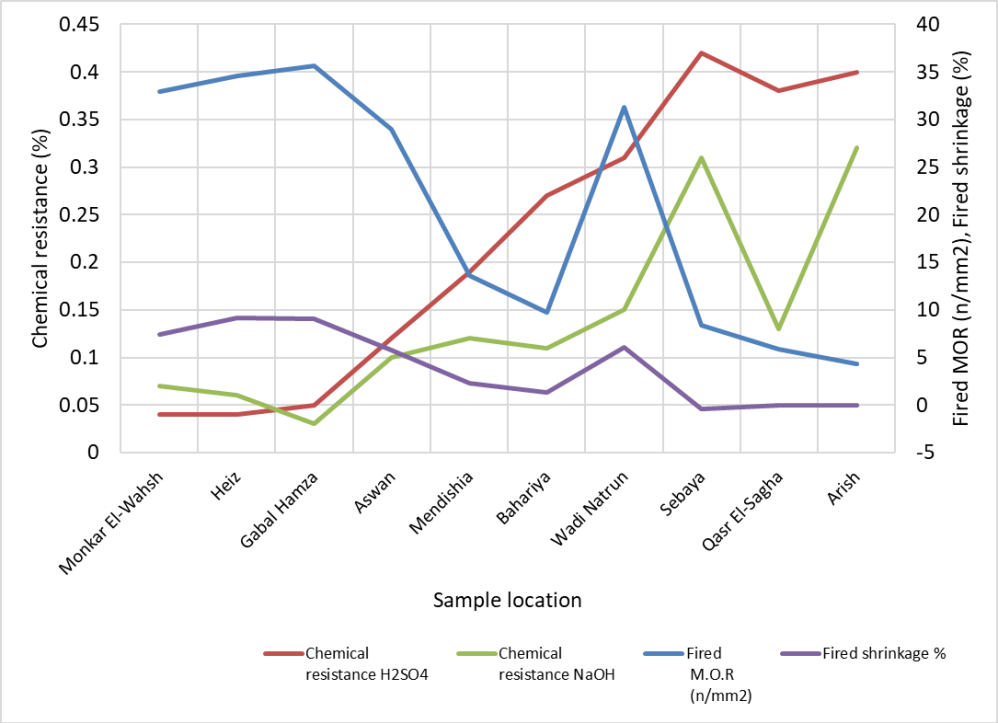

Fig.16. The relationship between the studied clay samples vs chemical resistance and modulus of rupture (MOR).

References

Abdel Wahab S., El-Belassy M., 1987. Sedimentology of the lower middle Miocene sequence in Gebel Hamza-Gebel um Qamar. Bulletin of Faculty of Science Cairo University 55 (2): pp. 445–480.

Abdou A.A., Shehata M.G., 2007. Geochemical Study of the Shales of Gebel Ghorabi Member, Bahariya Oasis, Western Desert, Egypt. Australian Journal of Basic and Applied Sciences, 1 (4): pp. 553-560.

Abu Al-Izz M.S., 1971. Landforms of Egypt. The American University in Cairo press. P. 11.

Anggono J., 2005. Mullite ceramics: its properties structure and synthesis. Jurnal Teknik Mesin, 7(1), pp. 1-10.

Bain D.C., Smith B.F.L., 1987. Chemical Analysis; In: A Handbook of Determinative Methods in Clay Mineralogy, Wilson, M.J. (Ed). pp. 248-274.

Beadnell H.J.L., 1905. The relations of the Eocene and Cretaceous system in the Esna-Aswan reach in Nile Valley- Quort. J. Geol. Soc. London.61, pp. 667-678.

Bish D.L., Reynolds R.C., Jr. 1989. Sample Preparation for X-ray diffraction. MSA Reviews in Mineralogy V. 20, pp. 73-97.

Brown G., Brindley G.W., 1980. Crystal structures of clay minerals and their X-ray identification. Mineralogical Society, London, pp.361-410.

Chavez C.L., Johns W., 1995. Mineralogical and ceramic properties of refractory clays from central Missouri (USA). Applied Clay Science Volume 9, Issue 6, June 1995, pp. 407-424.

Dechaine G.P., Gray M.R., 2010. Chemistry and association of vanadium compounds in heavy oil and bitumen, and implications for their selective removal. Energy and Fuels, 24(5), pp. 2795-2808.

Ekosse G., 2001. Provenance of the Kgwakgwe kaolin deposit in Southeastern Botswana and its possible utilization. Appl. Clay Sci. 20, pp. 137-152.

El-Askary M.A., 1972. Mineralogical and geological studies on some Egyptian kaolins. Unpublished Ph.D. dissertation Alexandria University.

Garver J.I., Royce P.R., Scott, T.J., 1994. The presence of ophiolites in tectonic highlands as determined by chromium and nickel anomalies in synorogenic shales: two examples from North America. Russian Geol. Geophys.35, pp. 1-8.

Gill J., 1981. Organic Andesites and Plate Tectonics. Springer-Verlag, Berlin, 390 P.

Grim R.E., 1951. Method and Application of Differential Thermal Analysis. Annals of the New York Academy of Sciences, 53: pp. 1031–1053. https://doi:10.1111/j.1749-6632.1951.tb48880.x.

Grim R.E., 1968. Clay Mineralogy. New York: McGraw-Hill, 596 P.

Grim R.E., Bradley W.F., 1940. Investigation of the effect of heat on the clay minerals illite and montmorillonite. Journal of the American Ceramic Society, 23 (8), pp. 242-248.

Gromet L.P., Dymek R.F., Haskin L.A., Korotev R.L., 1984. The North American shale composite. Its compilation, major and trace element characteristics. Geochim. Cosmochim. Acta 48, 2469-2482. Hantar G., 1990. North Western Desert. In: The Geology of Egypt (Ed. R. Said), chapter 15, pp. 293-319.

Hendriks F., Luger P., Bowitz J., Kallenback H., 1987. Evolution of depositional environments of SE-Egypt during the Cretaceous and Lower Tertiary. - Berl. Geowiss. Abh., (A), 75, pp. 49 –82, Berlin.

Hughes C., Russell J., Robbins T.W., 1994. Evidence for executive dysfunction in autism. Neuropsychologia, 32, pp. 477-492.

Hunziker J.C., 1966. On the geology and geochemistry of the area between Valle Antigorio and Valle di Campo (Ticino). -Swiss Mineralogical and Petrographic Communications 46 (2), pp. 473-552.

Issawi B., 1969. Geology of Kurkur - Dungul area, - Egypt, Geol. Surv., paper no. 46, 102 P.

Issawi B., 1971. On the Nubia sandstone. Bull. A.A.P.G., Vol. 55, pp. 891-893.

Issawi B., Fahmy N., 1975. An occurrence of post Maastrichtian quartz vein, Western Desert. Egypt, J. Geol., Vol. 19, No. 2, pp. 54-57.

Knauer G.A., Martin J.H., 1973. Seasonal variation of Cd, Co, Mn, Pb ad Zn in water and phytoplankton in Monterey bay, California. - Limnol. Oceanogr., Milwaukee, 18, pp. 597- 604.

Kumari N., Mohan, C., 2021. Basics of clay minerals and their characteristic properties. Clay Clay Miner, 24, pp. 1-29.

McCulloch M.T., Wasserburg G.J., 1978. Sm-Nd and Rb-Sr chronology of continental crust formation: Science, 200, pp. 1003-1011.

Millot G., 1970. The geology of the clays. Springer- Verlag, 429 P.

Moore D.M., Reynolds R.C. Jr., 1997. X-ray diffraction and the identification and Analysis of clay minerals: Oxford University Press, Inc., New York, New York, 378 P.

Newman A.D.C., 1987. Chemistry of clays and clay minerals; Longman scientific and technical; USA.

Okunlola O.A., Idowu O., 2012. The geochemistry of claystone-shale deposits from the Maastrichtian Patti formation, Southern Bida basin, Nigeria. Earth Sci. Res. SJ. Vol. 16, No. 2 (December 2012): pp. 139-150.

Olusola J., Suraju A., Nurudeen A., 2014. Geochemical and Mineralogical Studies of Kaolinitic Clays in Parts of Ilorin, Southwestern Basement Rock Area, Nigeria. Universal Journal of Geoscience 2: pp. 212-221

Parham W.E., 1966. Lateral variations of clay mineral assemblages in modern and ancient sediments. L. Heller and A. Weiss, eds., Israel Prog. Sci. Trans. Int. Clay Conf., Jerusalem, 1966, 1: pp. 135-146.

Pettijohn F.J., 1957. Sedimentary Rocks. 3rd Edition, Harper Co. New York, 628 P.

Pettijohn F.J., 1975. Sedimentary Rocks. – 3rd Ed., 628 P., New York (Harper & Row).

Prevot L., 1990. Geochemistry, Petrography, Genesis of Cretaceous-Eocene Phosphorites. The Ganntour Deposit (Morocco): a type example. Ph.D. Thesis, University Louis Pasteur, Strasbourg.

Riley K.W., Saxby J.H., 1983. Association of organic matter and vanadium in oil shale from the Toolebuc Formation of the Eromanga Basin, Australia. Chem. Geol., 37 P.

Said R., 1962. The Geology of Egypt. Elsevier Publishing Company. Amsterdam –New York.

Sharma G.D., 1979. The Alasken Shelf. Spriger-Verlag, New York.

Stromer E., 1914. Die topographie und geologie der strecks Gharag Baharije nebst Ausfuhrungen, uber die geologische Geschichte Agyptens Abhandl. Konig. Bayerische Akademie der Wissenschafte Mat. Phus. Klasse. Band XXIV Abheilung II, pp. 1-78.

Taylor S.R., McLennan S.M., 1985. The Continental Crust: Its Composition and Evolution. An Examination of the Geochemical Record Preserved in Sedimentary Rocks [M]. 312 P., Blackwell Sci, Oxford.

Turekian K.K., Wedepohl K.H., 1961. Distribution of the elements in some major units of the Earth's Crust. Geol. Soc. Am. Ball., 72, pp. 175-192.

Wahid A., 2020. Geological studies on the raw materials used in the preparation of the mix composition of sewage pipes, from some Egyptian localities, Ph.D. Thesis, Al-Azhar University, Cairo, Egypt.

Wycisk K., 1987. Contribution to the subsurface geology of the Misaha trough and the Southern Dakhla Basin. Ber